

UNIVERSITÀ
DEGLI STUDI
DI PADOVA



UNIVERSITY OF PADOVA

DEPARTMENT OF MEDICINE – DIMED

In collaboration with the **Medical University Gdansk**

International PhD Program: ARTERIAL HYPERTENSION AND
VASCULAR BIOLOGY
(XXVII CYCLE)

Detection of KCNJ5 mutations in the APA tissues
and cell-free DNA with a novel Taqman-based
approach

Coordinator: Ch.mo Prof. Gian Paolo ROSSI, MD

Supervisore: Ch.ma Dott.ssa. Teresa Maria SECCIA, MD

PhD Student :Daniela Cangiano

ACADEMIC YEAR 2013/2014

Abstract

Background: Primary aldosteronism (PA) is the most common endocrine form of secondary arterial hypertension with an estimated prevalence of ~ 11.2% in patients referred to specialized centers and 4% in primary care, but as high as 50% in patients with resistant hypertension. The two main forms of PA are: aldosterone-producing adenoma (APA), surgically curable with the removal of adenoma that is able to overproduce aldosterone, and bilateral adrenocortical hyperplasia (BAH), which needs drug therapy. About ~ 30% APAs have somatic mutations in KCNJ5 gene that encodes for the potassium channel (KIR3.4), which plays a crucial role in the maintenance of the cell membrane by pumping potassium (K^+) out of the cells, thereby producing a negative membrane potential. The KCNJ5 channels that contain G151R, T158A, or L168R mutations cause membrane permeability to Na^+ , resulting in Na^+ entry, cell depolarization, constitutive aldosterone production, and cell proliferation.

The standard approach used to detect the mutations in KCNJ5 gene is sequencing of DNA extracted from adrenal tissue of hypertensive patients with lateralized excess in aldosterone production. However, DNA sequencing is a time consuming and rather expensive technique not feasible in all standard laboratories.

Aims of our study were 1) to develop a strategy for genotyping DNA extracted from the adrenal tissue, which exploited a TAQ-MAN based PCR technology; 2) to evaluate if such Taq-Man-base technology allows detection of KCNJ5 mutations in the adrenal tissue and cf-DNA isolated from peripheral blood.

Methodologic Approach:

1. Development of a novel strategy based on Taq-man probe to detect KCNJ5 mutations
2. Development of a protocol to isolate cf-DNA from blood collected in the inferior vena cava and adrenal veins.
3. Measurement of cf-DNA concentration and assessment of its fragmentation.
4. Identification of KCNJ5 mutation in cf-DNA

Results: By applying the novel technology based on Taq-man probe we correctly identified 30 mutated patients in a cohort of 50 consecutive APA patients, with no misclassification.

After isolating cf-DNA from the adrenal veins and inferior cava blood, and measuring its concentration, we evaluated cf-DNA fragmentation with the integrity index in 24 samples. Integrity index < 1 suggested that cf-DNA was released from the adrenal tissue through an apoptotic mechanism. HRM analysis of cf-DNA isolated from adrenal blood allowed us to identify the KCNJ5 mutation in the APA side.

Conclusions and perspectives: The novel technology based on Taq-man probe allowed detection of all mutated patients in the examined cohort of APA patients, thus proving that this strategy could be used as an alternative to DNA sequencing. The results of our study also showed the feasibility to isolate cf-DNA from small amount of blood collected from the adrenal veins, and suggested that KCNJ5 mutations may be detected in cf-DNA. However, this approach needs to be verified for feasibility and accuracy in a larger population.

If confirmed, analysis of cf-DNA isolated from the peripheral venous blood could be helpful for an early detection of KCNJ5 mutations and therefore for the selection of PA patients to be submitted to adrenal vein sampling.

Furthermore, this strategy could be also useful for detecting KCNJ5 germline mutations responsible for the rare hereditary form of hyperaldosteronism FH-3.

Riassunto

Background. L'Iperaldosteronismo primario (PA) è la forma endocrina più comune d'ipertensione arteriosa secondaria con una prevalenza stimata di circa il 4% nella popolazione generale e dell'11% nei pazienti che afferiscono ai centri di riferimento per l'ipertensione. Nei pazienti con ipertensione resistente la prevalenza del PA è stimata pari al 50%, mostrando che tale patologia non è così rara come ritenuto in passato.

Le due forme principali di PA sono l'adenoma produttore aldosterone (APA), caratterizzato da iperproduzione lateralizzata di aldosterone, e l'iperplasia surrenalica bilaterale (BAH). La distinzione tra le due forme è di cruciale importanza poiché la prima richiede terapia chirurgica, mentre la seconda terapia medica. Considerando che la rimozione dell'APA determina la correzione del quadro biochimico-clinico di PA e la cura o il miglioramento dell'ipertensione, il riconoscimento dell'APA è fondamentale per offrire una *chance* di guarigione dell'ipertensione o di miglioramento del controllo dei valori pressori ai pazienti che ne sono affetti.

Il 40% degli APA presenta mutazioni somatiche nel gene *KCNJ5* che codifica per il canale del potassio KIR 3.4. Questo canale gioca un ruolo fondamentale nel mantenimento del potenziale di membrana pompando il K^+ al di fuori della cellula, provocando in tal modo un potenziale di membrana negativo. Allorquando il gene *KCNJ5* contiene le mutazioni G151R, T158A o L168R il canale KIR 3.4 acquisisce capacità di condurre Na^+ all'interno della cellula. Gli effetti della mutazione a livello della cellula sono depolarizzazione cronica, produzione costitutiva di aldosterone e proliferazione cellulare.

L'approccio attualmente in uso per identificare tali mutazioni è il sequenziamento, secondo Sanger, del DNA estratto dal tessuto surrenalico rimosso durante surrenectomia nei pazienti con PA e iperproduzione lateralizzata

di aldosterone. Il sequenziamento del DNA, tuttavia, è costoso , richiede tempo e non è disponibile di routine in tutti i laboratori.

Scopo generale dello studio è stato quello di sviluppare una strategia alternativa al sequenziamento fondata sull'uso delle sonde Taq-man in Real Time PCR (Q-PCR) per il rilevamento di mutazioni KCNJ5 nel tessuto surrenalico e nel DNA circolante (cell-free DNA, cf-DNA) isolato da sangue periferico. Lo sviluppo di questa metodologia potrebbe semplificare notevolmente l'identificazione delle mutazioni KCNJ5 negli APA e, infine, permetterne la detezione nel DNA del sangue circolante.

In sintesi, l'approccio metodologico include:

sviluppo di una nuova strategia basata sull'utilizzo delle sonde Taq-man per rilevare le mutazioni nel gene KCNJ5.

Sviluppo di un protocollo per isolare il cf-DNA da sangue delle vene surrenaliche e dalla vena cava inferiore.

Misurazione della concentrazione del cf-DNA valutandone la sua frammentazione.

Identificazione di mutazioni nel gene KCNJ5 a partire dal cf-DNA

Risultati. Applicando la tecnologia sviluppata nel nostro laboratorio, basata sulle sonde Taq-man, sono stati identificati correttamente 30 pazienti mutati in una coorte di 50 pazienti APA consecutivi, senza errori di classificazione.

Dopo aver isolato il cf-DNA dal sangue delle vene surrenaliche e dalla vena cava inferiore, e misurato la sua concentrazione, abbiamo valutato la frammentazione del cf-DNA in 24 campioni con l'indice di integrità.

I bassi valori dell'indice d'integrità riscontrati nei cf-DNA isolati da sangue venoso surrenalico suggeriscono che la ghiandola surrenalica rilasci per apoptosi frammenti di DNA. L'analisi HRM dei cf-DNA isolati dal sangue delle vene surrenaliche di un paziente con un APA sinistro contenente la mutazione L168R ha permesso d'identificare correttamente la mutazione nel cf-DNA isolato dalla vena surrenalica sinistra.

Conclusioni e prospettive. La tecnologia basata sulle sonde Taq-man ha permesso d'identificare, senza errori di misclassificazione, in una coorte di 50 pazienti con APA, tutti i 30 pazienti che presentano una mutazione del gene KCNJ5. Tale strategia, pertanto, potrebbe rappresentare un'alternativa alla ben più lunga e complessa tecnica basata sul sequenziamento del DNA. I risultati del nostro studio hanno anche mostrato che è possibile isolare il cf-DNA da esigue quantità di sangue raccolto dalle vene surrenaliche permettendo l'identificazione delle mutazioni KCNJ5 usando il cf-DNA tramite approccio combinato sonde Taq-man e analisi HRM. Quest'ultimo approccio, che prevede l'uso del cf-DNA richiede, tuttavia, conferma in un ampio numero di soggetti. La stessa strategia potrebbe anche essere impiegata in futuro per la rilevazione di mutazioni germinali KCNJ5 responsabili della nota forma ereditaria d'iperaldosteronismo FH-3

Summary

Introduction.....	9
Primary Hypertension	10
Secondary Hypertension	10
Adrenal glands and Aldosterone byosynthesis	11
HIstory of Primary Aldosteronism (PA).....	16
Diagnosis of PA.....	17
Subtype of PA.....	19
Adrenal Vein Sampling (AVS).....	20
Diagnosis of Aldosterone Producing Adenoma (APA).....	23
Genetic alteration in the development of APA.....	24
Somatic mutations in KCNJ5 gene in aldosterone-producing adenoma (APA)...	24
Somatic mutations in ATP1A1	27
Somatic mutations in ATP2B3	30
Somatic mutations in CACNA1D.....	31
Familial hyperaldosteronism type I (FH-1)	32
Familial hyperaldosteronism type I (FH-2)	34
Familial hyperaldosteronism type I (FH-3)	35
Germline mutations in CACNA1D cause primary aldosteronism.....	36
Circulating DNA as a promised biomarker for early diagnosis of Aldosterone Producing Adenoma	37
Circulating DNA: a promised of biomarker for early diagnosis of APA	37
Origin of circulating-DNA: cell apoptosis and necrosis.....	39
Aims.....	41
Flowchart	42

Material and methods	43
DNA Extraction from APA tissue	43
Taq-Man probe	44
Gradient curve.....	46
Real time PCR (Q-PCR).....	46
Allelic discrimination by Genotype Assignments	47
Sanger Sequencing.....	47
Collection of human plasma from adrenal veins and inferior cava	48
Circulating DNA (ct-DNA) extraction from plasma of APA patients	48
Plasma DNA concentration and integrity index	49
High resolution melting analysis (HRM).....	50
Protocol for PCR and HRM analysis.....	51
Statistical Analysis.....	51
Results	52
Identification of KCNJ5 mutations in the APA tissue with Taq-Man probe based technique.....	52
Allelic discrimination	58
Validation of new Taq-man based technique with Sanger Sequencing.....	59
Cell-free DNA isolation from plasma of Adrenal Vein Sampling	60
Calibration line for quantification of G151R 200 bp fragment	62
Calibration line for quantification of L168R 200 bp fragment.....	64
Calibration line for quantification of 400 bp fragment.....	66
Absolute quantification of circulating DNA.....	68
Evaluation of fragmentation through Integrity index	69
HRM analyses of DNA from APA tissue.....	70
HRM analyses of circulating DNA from AVS sample.....	72
Discussion	75
Conclusions	77
Bibliography	78

Introduction

Arterial hypertension (AH) affects 40% of the adult population in Europe and 1 billion people worldwide. According to the Centers for Disease Control and Prevention (CDC) and PAN American Health Organization (PAHO) it is called the “*silent killer*” because most people often have no symptoms.

Yet hypertension can lead to serious and sometimes even fatal conditions (Figure 1). Hypertension is the first risk factor for cardiovascular disease and death throughout the world. In particular, AH can be divided into two main types based on its cause: primary and secondary forms.

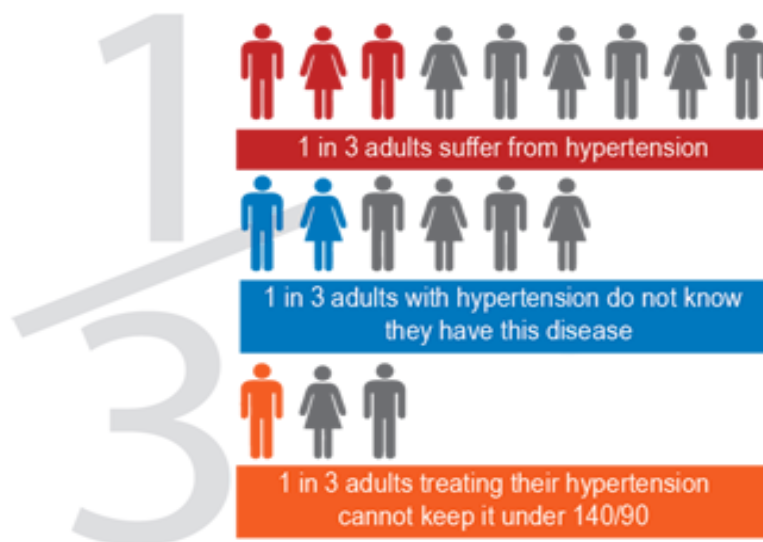


Figure 1: Prevalence of arterial hypertension in adult population (Data from Pan American Health Organization/World Health Organization, PAHO/WHO, 2013)

Primary Hypertension

This term defines a condition in which physicians are not sure what are the causes of this common form of high blood pressure. Primary hypertension is not directly attributable to any underlying condition, but it is caused by a combination of factors. The upward resetting of heart, vessels, and barostat functions, as well as the occurrence of vascular remodelling, represent the most important long-term cardiovascular alterations that are responsible for the maintenance of AH (Folkow B. 1993).

Secondary Hypertension

The prevalence of these forms, where a precise mechanism responsible for the elevation of blood pressure can be found, is not precisely known, albeit it is quite obvious that these forms are markedly underdiagnosed. These main forms are listed in figure 2.

Secondary cause	Prevalence ^a	Prevalence ^b	History	Screening	Clinical findings	Laboratory findings
Obstructive sleep apnoea	>5–15%	>30%	Snoring, daytime sleepiness, morning headache, irritability	Screening questionnaire; polysomnography	↑ neck circumference; obesity; peripheral oedema	Not specific
Renal parenchymal disease	1.6–8.0%	2–10%	Loss of good BP-control; diabetes; smoking; generalized atherosclerosis; previous renal failure; nocturia	Creatinine, ultrasound of the kidney	Peripheral oedema; pallor; loss of muscle mass	↑ Creatinine, proteinuria; ↓ Ca ²⁺ ; ↑ K ⁺ ; ↑ PO ₄
Renal artery stenosis	1.0–8.0%	25–20%	Generalized atherosclerosis; diabetes; smoking; recurrent flush pulmonary oedema	Duplex, or CT, or MRI, or angiography (drive by)	Abdominal bruits; peripheral vascular disease	Secondary aldosteronism: ARR →; ↓ K ⁺ ; ↓ Na ⁺
Primary aldosteronism	1.4–10%	6–23%	Fatigue; constipation; polyuria, polydipsia	Aldosterone–renin ratio (ARR)	Muscle weakness	↓ K ⁺ ; ARR ↑
Thyroid disease	1–2%	1–3%	<i>Hypert</i> thyroidism; palpitations, weight loss, anxiety, heat intolerance; <i>Hypo</i> thyroidism; weight gain, fatigue, obstipation	TSH	<i>Hypert</i> thyroidism: tachycardia, AF, accentuated heart sounds; exophthalmus; <i>Hypo</i> thyroidism: Bradycardia; muscle weakness; myxoedema	<i>Hypert</i> thyroidism: TSH ↓; fT4 and/or fT3 ↑; <i>Hypo</i> thyroidism: TSH ↑; fT4 ↓; cholesterol ↑
Cushing's Syndrome	0.5%	<1.0%	Weight gain; impotence; fatigue; psychological changes; polydipsia and polyuria	24 h urinary cortisol; dexamethasone testing	Obesity, hirsutism, skin atrophy, Striae rubrae, muscle weakness, osteopenia	24 h urinary cortisol ↑; Glucose ↑; Cholesterol ↑; K ⁺ ↓
Phaeochromocytoma	0.2–0.5%	<1%	Headache; palpitations; flushing; anxiety	Plasma-metanephrines; 24 h urinary catecholamine	The 5 'Ps': paroxysmal hypertension; pounding headache; perspiration; palpitations; pallor	metanephrines ↑
Coarctation of the aorta	<1%	<1%	Headache; nose bleeding; leg weakness or claudicatio	Cardiac ultrasound	Different BP (≥20/10 mmHg) between upper-lower extremities and/or between right–left arm; ↓ and delayed femoral pulsations; interscapular ejection murmur; rib notching on chest Rx	Not specific

Figure 2: The most common causes of secondary hypertension from European Heart Journal 2014

Primary aldosteronism (PA) is the most common endocrine cause of secondary hypertension with an estimated prevalence of 11.2% in referred patients to the specialized centers and 4% in primary care (Rossi GP et Al. 2006).

Prevalence is higher, up to 50%, in patients with resistant AH. PA includes a variety of disorders characterized by an overproduction of aldosterone, the principal mineralocorticoid steroid hormone of family produced in the adrenal glands.

Adrenal glands and aldosterone biosynthesis

The adrenal glands are located bilaterally in the retro peritoneum superior and slightly medial to the kidney (Figure 3). Each adrenal gland is composed of two distinct structures: the adrenal cortex and medulla. The adrenal cortex is composed of three concentric layers: zona glomerulosa, zona fasciculata, and zona reticularis (Figure 4). They were originally described in 1866 by Arnold, and have different cellular differentiation that accounts for the specificity of the steroid production.

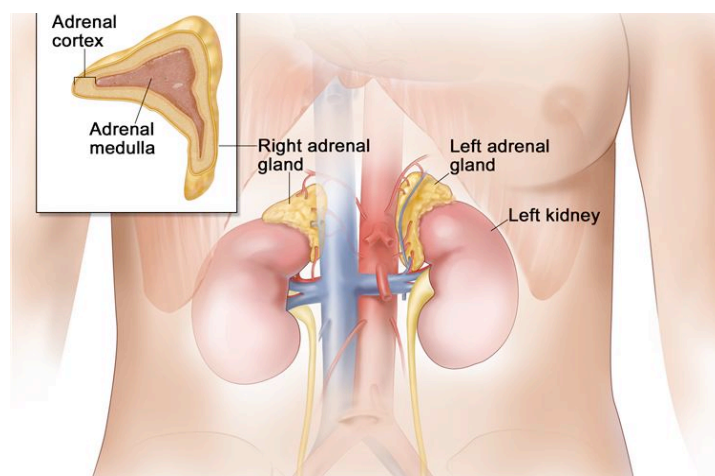


Figure 3: Anatomy of Adrenal Gland

(From National Cancer Institute, Teresa Winslow 2013)

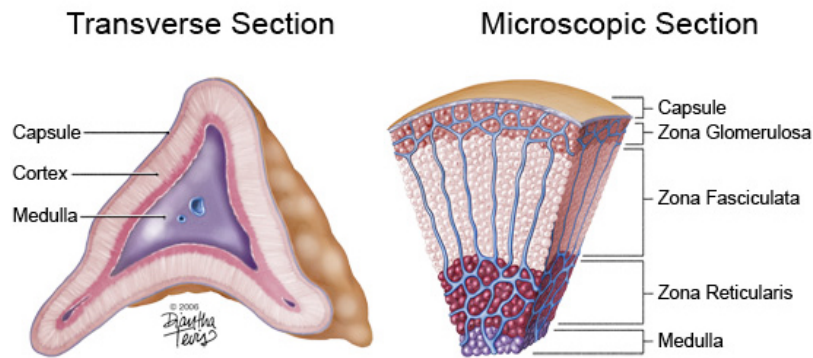
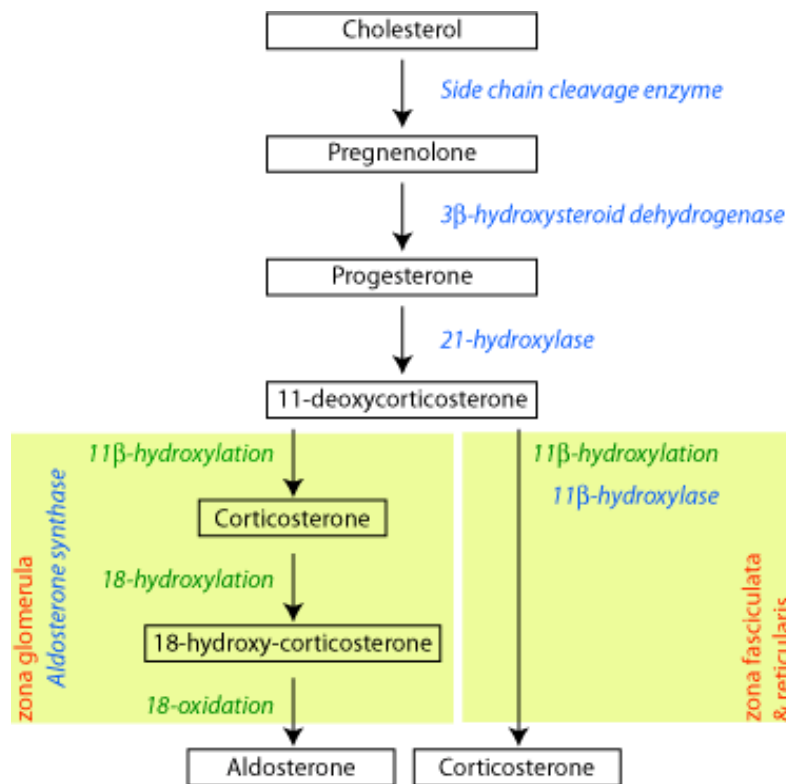


Figure 4: Adrenal Gland cross section
 (From website Department of Physiology of Georgia)

The zona glomerulosa (ZG) lies just beneath the adrenal capsule and it is composed of small clusters containing less cytoplasm than the other cortical cells. The zona fasciculata (ZF) forms broad bands of large cells with distinct membranes arranged in cords of about two cells wide. Their cytoplasm has numerous small lipid vacuoles that may indent the central nucleus and resemble lipoblasts; most cortical volume and lipid stores are depleted after ACTH surge. The zona reticularis is composed of organized cells that are smaller and thinner than zona fasciculata cells, and contain granular, eosinophilic cytoplasm and abundant lipofuscin, but only scarce lipids.

Aldosterone is secreted by ZG cells (Figure 4). Its synthesis needs a series of specific enzymatic reactions, the final steps of which are catalyzed by aldosterone synthase (encoded by *CYP11B2*). The *CYP11B2* gene shares a high degree of homology (95%) with the gene for 11 β -hydroxylase (*CYP11B1*), which catalyzes the final steps in cortisol biosynthesis in ZF (Figure 5). *CYP11B1* and *CYP11B2* genes are located in tandem on chromosome 8q21–22 (McMahon GT, et al 2004).



Legend: enzyme in blue, action performed in green, location in red.

Figure 5: Schematic Biosynthesis of Aldosterone

The main aldosterone secretagogues are angiotensin II (Belloni et al. 1996), potassium (K^+) and ACTH. In the basal state ZG cells are hyperpolarized (-78mV to -90 mV) because of background K^+ leakage that occurs essentially via TWIK (tandem pore domain K^+ channels), and in particular via TASK channels 1 and 3 that are outwardly rectifying channels sensitive to changes in extracellular pH (Figure 6). (Carey et al. 2012, Velarde-Miranda et al, 2013). Binding of angiotensin II to angiotensin II subtype 1 receptor (AT1R) blocks these leaky channels and other K^+ channels such as Kir3.4, as well as Na^+/K^+ ATPase, thus leading to glomerular membrane depolarization, activation of voltage-gated calcium channels (essentially low-voltage activated channels but also high-voltage activated channels) and calcium influx. Calcium is also released from intracellular stores via activation of phospholipase C (Hattangady NG et al, 2012). Changes in extracellular K^+ can also directly cause membrane depolarization and calcium entry (Beuschlein F et al 2013). Intracellular calcium stimulates aldosterone production by acting at multiple steps (Guagliardo NA, et al. 2012) by increasing:

1. The activity of cholesterol ester hydrolase, which de-esterifies cholesterol and thus releases it from its cytoplasmic storage sites.
2. The delivery of cholesterol to the outer mitochondrial membrane.
3. The transcription and translation of steroidogenic acute regulator protein (StAR), which in turn increases the intra-mitochondrial transfer of cholesterol to the inner membrane.
4. The mitochondrial oxidative metabolism and formation of the cofactors required for CYP11B2 activity, which in turn enhance the transcription of aldosterone synthase (Bassett MH et al. 2004).

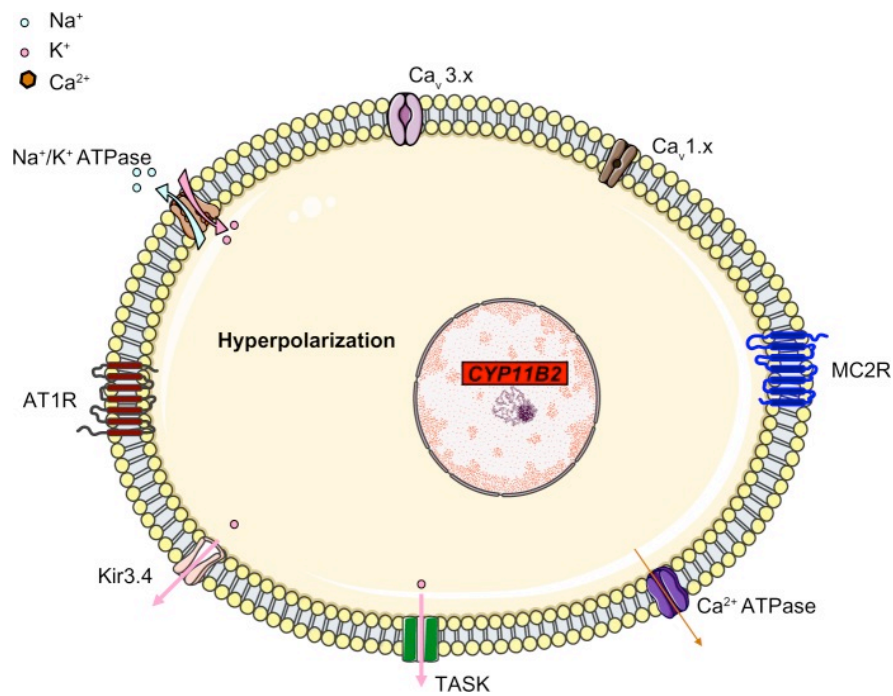


Figure 6: A simplified, schematic diagram of a ZG cell at rest, when the cell is hyperpolarized due to leaky K⁺ channels (TASK). Both Na⁺/K⁺ ATPase and Kir3.4 contribute to the maintenance of membrane hyperpolarization. The voltage-gated Ca²⁺ channels are represented in the closed form. (The Application of Clinical Genetics 2014)

History of Primary Aldosteronism (PA)

Dr. Jerome Conn was the first to well characterize the disorder (Coon and Louis, 1956) after a case report by Litynski in 1953 in a polish journal (Litynski, 1953). Conn presented the first case of PA during his presidential address at the Annual Meeting of the Central Society for Clinical Research in October 1954. Six months earlier Dr. Stefan Fajans asked to Dr. Conn to evaluate a 34-year-old woman with a 7-year history of muscle spasms, weakness, episodic paralysis and tetany, who was hypertensive for at least 4 years. Conn suspected, based on his prior research in sodium balance and acclimatization to tropical weather, which the patient suffered from excess production of the adrenal salt-retaining hormone. He found that her sweat chloride was essentially undetectable, supporting his hypothesis. Although Conn planned a bilateral adrenalectomy, the surgeon William Baum removed the right adrenal gland where a 13g tumor was found. After surgery, the metabolic and clinical abnormalities reversed almost completely. Conn could therefore establish a link between the autonomous overproduction of aldosterone released from the tumor and the symptoms complained by the patient. Since then, the syndrome has been termed Conn's syndrome (Rossi et Al. 2008) and the tumor producing excess aldosterone was defined as 'Conn's adenoma', a form that was replaced by used as synonym of aldosterone-producing adenoma (APA). The inappropriate production of aldosterone in PA causes suppression of plasma renin, Na^+ retention, K^+ excretion, and high blood pressure. However, due to a reset osmostat, serum sodium concentration tends to be high normal or slightly high in most PA patients, which is a useful clinical clue in PA. With time excess aldosterone levels also cause hypomagnesaemia and metabolic alkalosis. If severe, PA associated hypokalemia induces development of weakness, myalgias, muscle spasms, headaches, and arrhythmias. Less frequently, decreased ionized calcium and hypokalemic metabolic alkalosis cause overt tetany, as in Conn's index patient.

PA is also characterized by cardiovascular and renal damage (Rossi et Al. 1996), which is often more marked than that found in patients with essential hypertension and similar blood pressure values (Savard et al. 2013). Since correction of PA may prevent or reverse target organ damage, diagnosis of PA is of utmost relevance for preventing target organ damage.

Diagnosis of PA

Hiramatsu et al. introduced the aldosterone-to-renin ratio (ARR) as a screening test to identify PA in 1981. After then, ARR remains the cornerstone for diagnosing PA, as confirmed by the 2008 Guidelines of the International Endocrine Society. Two simultaneous blood tests are required to calculate ARR: the plasma (or serum) aldosterone concentration (PAC) and the plasma renin activity (PRA).

$$\text{ARR} = \text{PAC}/\text{PRA}$$

The ARR is a crude bivariate analysis; hence, its value depends on plasma aldosterone concentration (PAC) and on levels of renin. However, very different PAC and renin values can produce the same ratio. Moreover, the assays that are currently available for measuring plasma renin activity (PRA) and direct renin assay (DRA) lose their precision when levels of renin are low. As a result of this loss of sensitivity, and to avoid overinflating the ARR when levels of renin are very low, the lowest renin value that can be included in the ratio is often fixed at a minimum (which is 0.2 ng/ml per h for PRA).

Thus, rather than using the ARR purely arithmetically, the combination of an increased ARR and a PAC >416 pmol/l (15 ng/dl) should be used to detect patients with PA and regarded as indicative of this condition. Widely different cut-off values of ARR have been proposed for PA diagnosis. However, in the largest study published to date, which examined 126 consecutive hypertensive patients referred to 14 specialized centers for hypertension in Italy, by using the diagnosis of APA as the gold standard for identifying PA patients and the receiver operating characteristic (ROC) curves and the Youden index for the analysis, the ARR optimal cut-off was 26 (Rossi 2006). This value corresponded to a sensitivity of 80.5% and a specificity of 84.5%.

By definition a screening test must be highly sensitive to avoid that any patient(s) with PA is undetected. This requirement implies that the test often gives false-positive results that need to be identified before addressing the patients to the adrenal-vein sampling. This latter, as reported in detail below, may be risky. The oral sodium loading test, the saline infusion test, the captopril challenge test and the fludrocortisone with salt-loading test, are the tests currently used to exclude false positive results. The purpose of these tests is to demonstrate that the excess secretion of aldosterone is autonomous from the renin–angiotensin system. Unfortunately, these tests cannot provide unequivocal information because aldosterone secretion is dependent on angiotensin not only in patients with idiopathic hyperaldosteronism, but also in many patients with APA. Hence, if the ARR is properly determined, a notably raised value is a strong indication that the patient has PA.

Subtype of PA

The most common forms of PA are aldosterone-producing adenoma (APA) and bilateral adrenocortical hyperplasia (BAH), also referred to as idiopathic hyperaldosteronism (IHA). PA can be classified as surgically and not surgically curable:

1. Surgically curable:

- ❖ Aldosterone-producing adenoma (aldosteronoma, APA)
- ❖ Multinodular unilateral adrenocortical hyperplasia (MUAN)
- ❖ Pheochromocytoma causing Primary aldosteronism

2. Surgically not curable:

- ❖ Bilateral adrenal hyperplasia (BAH)
- ❖ Unilateral APA with BAH
- ❖ Familial hyperaldosteronism

The patients positive at the screening test should undergo imaging tests for identification of adrenocortical nodules and AVS to distinguish between unilateral and bilateral excess production of aldosterone (Rossi GP, et Al. 2006) (Rossi et Al. 2001). A high resolution CT scan with 2–3 mm cuts represents the best available technique for identifying adrenal nodules, which can be APA, primary unilateral adrenal hyperplasia or bilateral adrenal hyperplasia. Imaging is crucial to identify the rare but large aldosterone-producing carcinoma.

Half of APAs are <20 mm in diameter and up to 42% are <6 mm in diameter, therefore, most patients with primary aldosteronism attributable to an APA who can be cured with surgery have a small or very small tumour. Other surgically curable subtypes of primary aldosteronism, such as primary aldosteronism caused by primary unilateral adrenal hyperplasia or multinodular unilateral adrenocortical hyperplasia, have nodular lesions that are also most often very small (<10 mm in diameter), which makes them hardly detectable with CT or MRI. Hence, an imaging-guided strategy for subtype differentiation of PA would result in missing masses producing excess aldosterone and in revealing adrenal masses that are not APAs. Moreover, imaging is inadequate to achieve discrimination between APA and idiopathic hyperaldosteronism.

Adrenal Vein Sampling (AVS)

Patients with PA could have either bilateral (BAH) or unilateral (APA) adrenal disease (Chao CT et Al. 2013). Since unilateral and bilateral forms require different treatments, it is of crucial relevance to discriminate between them. In fact, unilateral forms can be treated by laparoscopic adrenalectomy, whereas bilateral forms need medical management with mineralocorticoid receptor antagonists. Of interest, surgery can normalize serum K⁺ concentrations in almost all PA cases, and cure or improve hypertension in more than 80% of cases with unilateral forms (Letavernier E et Al. 2008).

The Endocrine Society Guidelines claim adrenal vein sampling (AVS) as the gold standard to distinguish between unilateral from bilateral aldosterone hypersecretion (Funder JW et Al. 2008, Rossi GP et Al. 2014). However, since AVS procedure is technically demanding, and carries a tiny, but not negligible, risk of adrenal-vein rupture (Daunt N et Al. 2005, Rossi 2011) it is recommended only in PA patients who are eligible for surgical management.

AVS includes measurement of both aldosterone and cortisol in the inferior vena cava and adrenal veins. The measurement of cortisol, besides that of aldosterone, is essential for calculation of the selectivity index that confirms catheter placement and corrects for dilution during sampling (Figure 7).

Measurements of both steroids are also crucial for calculating the lateralization index, corresponding to PAC: PCC ratio on the dominant side over the PAC: PCC ratio on the contralateral side of the adrenal gland. Lateralization index provides an accurate diagnosis of PA with lateralized excess aldosterone production.

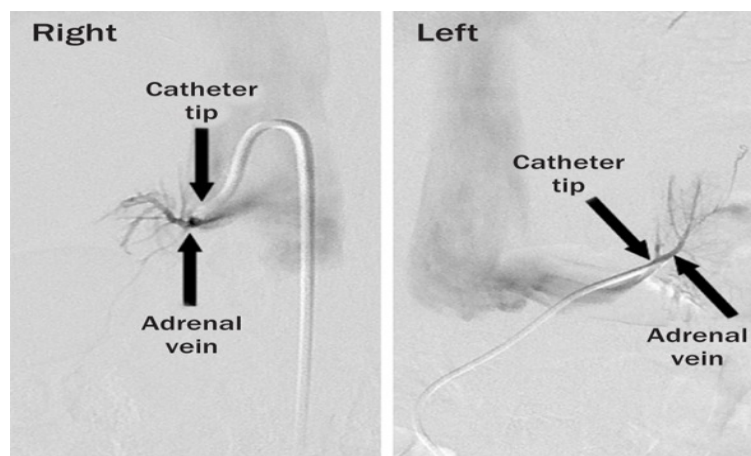


Figure 7: Placement of the catheter in the adrenal veins

(From website of Department of Radiology, Massachusetts General Hospital)

Some investigators also propose the use of the contralateral suppression index, defined by the aldosterone/cortisol concentration ratio of the non-dominant adrenal vein divided by the peripheral aldosterone/cortisol concentration ratio. (Rossi GP, et al. 2012). However, there are no evidence that suppression index provides more accuracy than lateralization index alone.

The performance of AVS and the interpretation of its results are generally regarded as challenging, (Stewart PM et Al. 2010) mainly due to the lack of accepted criteria to define selectivity of adrenal vein catheterization and lateralization of aldosterone excess (Rosenquist KJ, Dluhy RG. 2011). For these reasons and the recognized lack of reliability of alternative methods such as CT and biochemical tests for distinguishing unilateral from bilateral disease (Funder et Al. 2008) many patients with PA still undergoing adrenalectomy without prior demonstration of lateralized aldosterone excess. This practice can lead to unnecessary adrenalectomy and/or removal of the wrong adrenal in a substantial proportion of cases, as recently shown (Young WF, et Al. 2004, Kempers MJ, et AL 2009). Hence, development of new methods alternative to AVS could be very useful to support a certain diagnosis of PA

Diagnosis of Aldosterone Producing Adenoma (APA)

Identification of APA requires each of the following *four corner criteria* (Rossi et al Hypertension 2010):

- Evidence of PA at the screening test as defined above;
- Lateralization of aldosterone secretion at AVS
- Evidence of adenoma at pathology;
- Demonstration of normokalemia and cure or improvement of hypertension at follow-up after adrenalectomy.

Hence, after demonstration of lateralized excess aldosterone production, diagnosis of APA also requires evidence of a nodule at histology with ZG-or ZF-like cells, and correction of hypokalemia and cure or improvement of hypertension at follow-up after surgery. Histology and follow-up are therefore crucial issues for reaching a conclusive diagnosis of APA, which represents the only subtype of PA that can receive unequivocal diagnosis. Patients with biochemical evidence for PA but without conclusive evidence for lateralized aldosterone excess are presumed to have IHA.

*Genetic alteration in the development of
Aldosterone Producing adenoma (APA)*

Somatic mutations in KCNJ5 gene in APA

The *KCNJ5* gene, which is located on 11q24.3 chromosome, codes for Kir3.4, a member of the G-protein-activated inwardly rectifying potassium channel family (subfamily J, member 5). Kir3.4 is expressed in the ZG, where it forms a highly active heterotetramer with Kir3.1 (*KCNJ3*) that contributes to maintenance of the K⁺ equilibrium potential across the cell membrane. It also can form a homotetramer, which is less active than heterotetramer. Under physiologic conditions, both Kir3.4 and Kir3.1 draw K⁺ out of the cell thereby maintaining hyperpolarization of ZG membrane at rest. Selective transit of K⁺ through the channel pore is conferred by a GYG motif located at the narrowest part of the pore. This selectivity filter is very well conserved among different species and among the other channel in the family, supporting the concept of its crucial role. A loss-of-function mutation in *KCNJ5* was found to cause a rare form of long QT syndrome. (Yang Y, Yang Y, Liang B, et al. 2010). More recently, by using whole-genome sequencing to search for somatic mutations, Choi et al. found 2 recurrent mutations in 8 cases (38%) of a cohort of 22 APA patients. These mutations, corresponding to p.Gly151Arg (G151R) or p.Leu168Arg (L168R), occurred within or near the selectivity filter and altered the channel's selectivity. G151 constitutes the first glycine in the GYG motif, whereas L168's side chain abuts the side chain of the tyrosine in the same motif (Y152). *KCNJ5* channels that contain these mutations conduct Na⁺, with chronic depolarization, constitutive aldosterone production, and cell proliferation.

A novel mutation has been recently detected in our laboratory (Kuppusamy, et al, J Clin Endocrinol Metab 2014), characterized by threonine insertion before the selectivity filter of the K^+ channel. Such mutation causes loss of K^+ selectivity, Na^+ permeability and Ca^{2+} influx via opening of voltage calcium channels and impairment of Na^+/Ca^{2+} exchangers, leading to enhanced CYP11B2 expression and a constitutive over-secretion of aldosterone from the tumor (Figure 8).

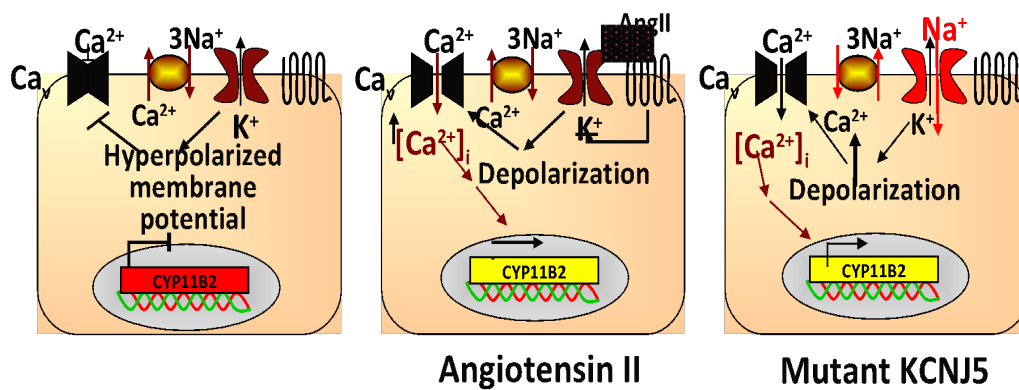


Figure 8: Activity of KIR 3.4 channel

Functional studies have confirmed that mutated *KCNJ5* can promote aldosterone synthesis: *CYP11B2* messenger RNA (mRNA) levels were found to be upregulated in APAs with *KCNJ5* mutations by a factor of 3.1 (compared to cells isolated from APAs without *KCNJ5* mutations) (Monticone S, et al. 2012). However, the mechanisms by which chronic Ca^{2+} stimulation activates aldosterone production in ZG cells remain unclear.

Visinin-like 1 (VSNL1, a neuronal calcium-sensor protein that participates to the transduction of calcium signaling) was found to be over-expressed in APAs harboring *KCNJ5* mutations. Increased expression of VSNL1 was suggested to protect the cells from calcium overload caused by the mutation. In fact, calcium overload can be dangerous for cell survival by promoting signaling pathways leading to death. (Williams TA, et Al. 2012).

Mulatero et al. also found a somatic p.Thr158Ala (T158A) mutation in an Italian patient with APA and a family history of PA. The same mutation had been reported in the original article by Choi et al but as a germline mutation. Threonine in position 158 is a well-conserved amino acid that forms hydrogen bonds with two conserved residues (P128 and C129) in the loop between the first transmembrane domain and the pore helix, and thus constrains the structure. The T158A mutation eliminates these hydrogen bonds thereby modifying channel selectivity. To date, only four other somatic mutations in *KCNJ5* have been reported in APA patients. Each mutation has been reported only once: a deletion mutation affecting isoleucine 157 (p.Ile157del), which is presumed to induce a conformational change near the selectivity filter; (Azizan EA et Al. 2012) two substitutions, which both affect the same amino acid (glutamic acid 145), p.Glu145Gln (E145Q) and p.Glu145Lys (E145K)(Azizan et Al. 2013), and a p.Trp126Arg (W126R) mutation. (Williams TA, Monticone S et Al. 2014).

Either (G151R) or (L168R) is present in 99% of *KCNJ5*-mutated APAs, whereas the five other mutations are extremely rare. *KCNJ5* somatic mutations are present in approximately 40% (range: 13%–65%) of APAs, thereby showing that they are more frequent than supposed some years ago (Boukroun S, Beuschlein F, Rossi GP, et Al. 2012). However, the proportion of APAs with *KCNJ5* mutations differs considerably from one center to another, reflecting disparities in the criteria used to differentiate unilateral from bilateral PA and to establish the diagnosis of APA.

The highest prevalence (65.2%) was found in a Japanese study. Of interest, studies from Japan report much higher prevalence of mutated APAs than that found in Western countries. (Taguchi R et Al. 2012).

Moreover, gender differences were also noticed: *KCNJ5* mutations are more frequent in women than in men. Nevertheless, the prevalence of *KCNJ5* mutations was higher in Japanese men than in women, thereby suggesting epidemiological marked differences between Japanese and Western populations.

Somatic mutations in ATP1A1

The *ATP1A1* gene encodes the alpha-1 (catalytic) subunit of the Na⁺/K⁺ ATPase, a member of the P-type ATPase family. It maps to chromosome 1p13.1 and comprises 10 transmembrane segments (from M1 to M10). There are two functionally important cytoplasmic loops: a large loop between M4 and M5 (which binds ATP) and a small loop between M2 and M3 (which has a key role in energy transduction). Upon activation, the transmembrane segment M1 interacts and cooperates with segment M4 to facilitate ion binding. For each ATP hydrolyzed, the Na⁺/K⁺ ATPase transports two K⁺ ions into the cell and three Na⁺ ions out of the cell. The resulting potassium and sodium gradients contribute to the resting membrane potential and action potentials. *ATP1A1* is strongly expressed in the ZG and to a lesser degree in the ZF. Recently, Beuschlein et al. performed exome sequencing of tumor and matched control tissue samples from nine males affected with hypokalemic PA and bearing wild-type Kir3.4. They found that three patients had somatic *ATP1A1* mutations: substitution of the leucine in position 104 (in M1) p.Leu104Arg (L104R) in two cases and substitution of the valine in the position 332 (in segment M4) p.Val332Gly (V332G) in the third case. Both amino acids are highly conserved among species and among different members of the P-type ATPase family.

Beuschlein et al then sequenced the entire coding region of *ATP1A1* in an additional 100 APAs and detected six cases with somatic mutations: four had the L104R mutation, while the other two featured a five amino acid deletion (p.Phe100_Leu104del). Targeted sequencing of the affected genomic locations was performed in 199 additional APAs and confirmed that *ATP1A1* mutations are present in 5.2% of patients with APA. (Beuschlein F et al. 2013). The sequencing data indicated that both wild type and mutated alleles were present in tumor tissues suggesting that the mutation was heterozygous. All mentioned alterations in the *ATP1A1* gene disrupt the glutamic acid in position 334 (site II), which is crucial for sodium and potassium ion binding and gating of the binding pocket. Beuschlein et al. also examined the functional impact of the *ATP1A1* mutations and found that mutated *ATP1A1* have impaired activity. Adenoma cells with an *ATP1A1* mutation showed substantially higher levels of depolarization. Hence, the mutations in *ATP1A1* change the transport mode from active pumping (three Na⁺ outwards and two K⁺ inwards) to passive conduction (inward current due to protons or Na⁺ ions, depending on the mutation) (Figure 9). This impairment in conduction leads to membrane depolarization, opening of voltage-gated calcium channels, increased intracellular calcium and thus increased *CYP11B2* expression with aldosterone hyper-production.

A new somatic mutation (p.Gly99Arg, G99R) has been recently reported. Glycine 99 interacts with isoleucine 292 to mediate the opening of the gate at the entrance of the binding pocket, while Arginine in the position 99 alters the surrounding structure (Williams TA et Al. 2014).

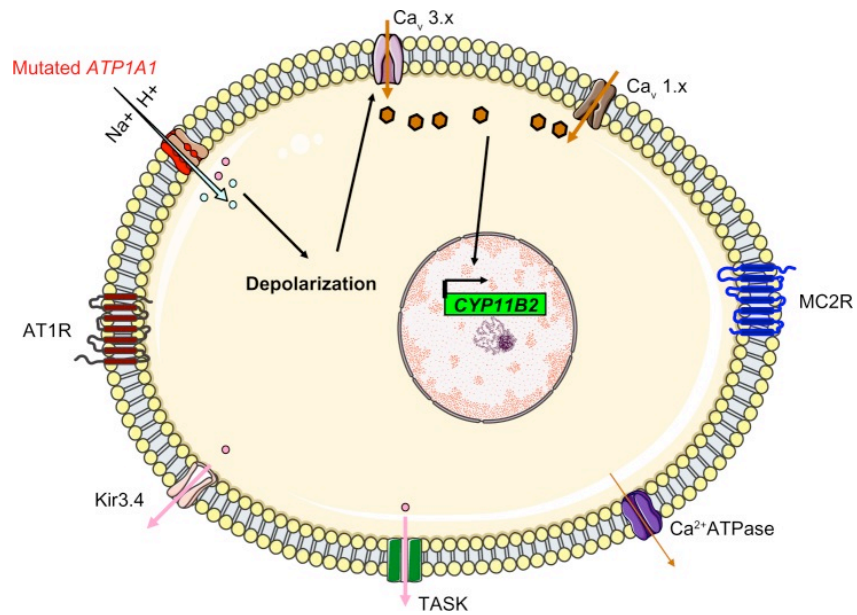


Figure 9: The molecular mechanisms underlying hyperaldosteronism in patients with *ATP1A1* mutations. The Na^+/K^+ ATPase changes from actively pumping (3 Na^+ outwards and 2 K^+ inwards) to passive conduction of an inward current (protons or Na^+ ions, depending on the mutation)(From website *The applications of Clinical Genetics* 2014)

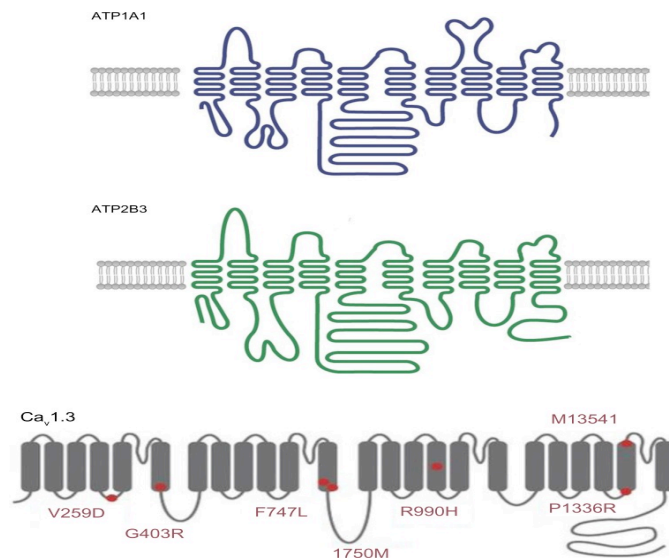


Figure 10: A schematic diagram of the structure of Na^+/K^+ ATPase subunit alpha 1 (upper panel, ATP1A1), Ca^{2+} ATPase 3 (middle panel, ATP2B3) and the alpha subunit of low-voltage activated calcium channel Cav1.3, with known mutations indicated by red circles (lower panel). (*Nature Genetics*, Beuschlein F, Boulkroun S, Osswald A, et al. 2013)

Somatic mutations in *ATP2B3*

The *ATP2B3* gene encodes the plasma membrane calcium transport ATPase 3 (PMAC3), another member of the P-type ATPase family. Its structure is similar to that of *ATP1A1*, with 10 transmembrane segments and two functionally important cytoplasmic loops (Figure 9). *ATP2B3* is required for clearing calcium from the cytoplasm of eukaryotic cells and thereby has an important role in intracellular Ca^{2+} homeostasis. *ATP2B3* is located on the X chromosome (Xq28) and is expressed throughout the adrenal cortex. Beuschlein et al. reported three different in-frame deletions that resulted in either p. Leu425_Val426del or p. Val426_Val427del. These deletions affect a highly conserved residue and thus alter the M4 transmembrane helix in a region that is thought to be crucial for calcium ion binding. A functional study confirmed that *ATP2B3* mutations impair activity and inactivate pump function: cultured adenoma cells with an *ATP2B3* mutation showed substantially higher levels of depolarization. Another mutation consisting in a deletion (c.1281_1286delGGCTGT) had been recently reported. Several studies have shown that *ATP2B3* mutations have lower prevalence than *KCNJ5* in APA patients (0.9%–1.6%), and also that they are associated with severe forms of PA and are more common in men than in women. APAs with ATPase mutations were found to be smaller than APAs with *KCNJ5* mutations. Of interest, *KCNJ5* mutations were never found associated with *ATP1A1* or *ATP2B3* mutations in the same tumor.

Somatic mutations in CACNAID

The *CACNAID* gene encodes Cav1.3, the alpha subunit of an L-type voltage-gated calcium channel. This family of channels is characterized by sensitivity to dihydropyridine calcium channel blockers, which act as weak antagonists of Cav1.3. High-voltage-gated calcium channels differ from low-voltage-gated calcium channels (T-type channels) in terms of the voltage dependence of opening and inactivation and the kinetics of closure and inactivation. Cav1.3 is composed of four homologous repeats (I–IV), each of which has six transmembrane segments (S1–S6) and a membrane-associated loop between S5 and S6 (Figure 10). The channel's pore is formed by the S5, S6 and the loop. The *CACNAID* gene is located on 3p14.3. Alternative splicing gives rise to many different isoforms. *CACNAID* is expressed in the ZG and in many other tissues (heart, neurons, cochlear hair cells). By performing exome sequencing, Scholl et al. found two somatic mutations in *CACNAID* in 18 cases of APA. Both mutations affected well-conserved amino acids (p. Gly403Arg and p. Ile770Met) located at the cytoplasm ends of the S6 segment of repeats I and II. When expressed in HEK293T cells, both mutant genes were found to be associated with peak current amplitudes at less depolarized potentials, suggesting that mutations lead to channel opening at lower potentials. Scholl et al. sequenced all S6 segments in an additional 46 APAs, and they identified three additional somatic mutations. Easier activation of the mutant channels resulted in increased Ca²⁺ entry and greater aldosterone production. These mutations more frequently occur in males than in women, and are also more frequent in small than large APAs. Whether the smaller dimension of the APA is related to the abundance of ZG-type cells, which are lipid-poor and smaller than lipid-rich ZF-type cells, remains to be confirmed (Brown MJ et Al. 2014).

Familial hyperaldosteronism type 1 (FH-1)

In 1966, Sutherland et al. described the case of a father and son with hypertension due to hyperaldosteronism that was relieved by dexamethasone treatment. Familial hyperaldosteronism type I (called as FH-I according to the new nomenclature, Lenzini L et Rossi GP 2015) is also known as glucocorticoid-remediable aldosteronism (GRA) and is characterized by severe, early-onset hypertension. Although GRA accounts for less than 1% of patients with PA, it is considered to be the most common form of monogenic hypertension. Patients with GRA have an elevated risk of early haemorrhagic stroke and secrete high levels of hybrid steroids (18-hydroxycortisol and 18-oxocortisol). Glucocorticoid-remediable aldosteronism is inherited as an autosomal, dominant trait. The molecular etiology of GRA was characterized in 1992 and is based on unequal crossing-over between the 11 β -hydroxylase (*CYP11B1*) and aldosterone synthase (*CYP11B2*) genes, which results in a chimeric gene that combines the 5' promoter region of the 11 β -hydroxylase with the coding region of aldosterone synthase (Figure 11). The final effect is that aldosterone synthesis is regulated by ACTH (rather than by the renin-angiotensin system) and has a circadian rhythm similar to that of cortisol. This aberrant regulation explains why dexamethasone administration reduces aldosterone levels and normalizes blood pressure levels. GRA can be easily diagnosed with a polymerase chain reaction-based assay and, therefore, dexamethasone suppression test and hybrid steroid assays are no longer required. The Endocrine Society recommends genetic testing in patients with confirmed PA before the age of 20 and in those who have a family history of PA or strokes at a young age.

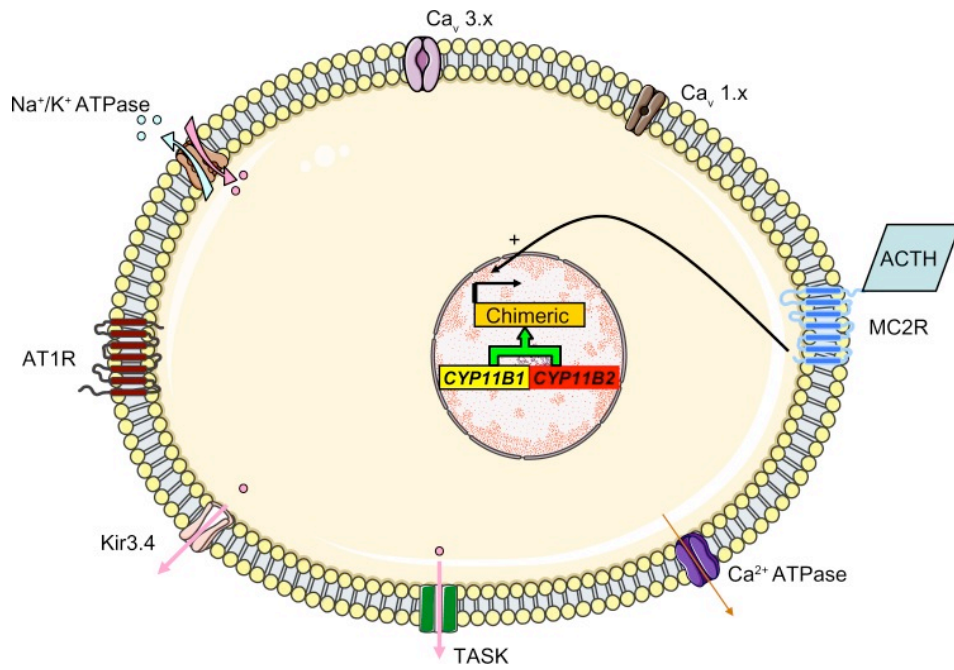


Figure 11: The molecular mechanism underlying GRA. Unequal crossing-over between the 11 β -hydroxylase (*CYP11B1*) and aldosterone synthase (*CYP11B2*) genes results in a chimeric gene and the control of aldosterone secretion by ACTH. (From *The Application of Clinical Genetics*, 2014)

Familial hyperaldosteronism type 2 (FH-2)

In 1992, Stowasser et al (Stowasser M et Al. 1992) described a second form of hereditary hyperaldosteronism in 13 patients with PA from 5 families. Because this form of PA did not respond to glucocorticoid treatment, genetic test for FH-1 was performed. The test showed lack of the chimeric gene, leading to identification of a novel syndrome that was classified as familial hyperaldosteronism type 2 (FH-2) (OMIM: 605635) only because of the familial occurrence (Lenzini L et Rossi GP 2015). FH-2, which comprises both adrenocortical hyperplasia and/or APA, is clinically undistinguishable from sporadic primary aldosteronism. The true prevalence of this form is not known, but is supposed to be as high as 6% in patients with PA. FH-2 is transmitted in an autosomal dominant fashion and although linkage analysis identified a quantitative trait locus (QTL) on chromosome 7p22 the responsible gene(s) remain unknown.

Familial hyperaldosteronism type 3 (FH-3)

In 2008 a third form of familial hyperaldosteronism was described. Hypertension was refractory to combination therapy in all three members of a family for which genetic test ruled out GRA as the cause of the clinical picture. Members of this family developed severe hypertension in childhood (before the age of 7), severe hypokalemia, and PA with very high levels of hybrid steroids (18-oxocortisol and 18-hydroxycortisol). The excised adrenals revealed a thin, atrophic ZG, a slightly decreased zona reticularis, and diffuse hyperplasia of the ZF (Geller DS et Al. 2008). The genetic basis of this syndrome was discovered three years later, when a germline heterozygous T158A mutation in *KCNJ5* was found in all affected members. Oki et al. demonstrated that expression of the T158A mutant in HAC15 cells caused increased Na⁺ inflow, higher plasma membrane voltage, increased intracellular calcium levels with enhanced aldosterone production. Cell proliferation was lower in the T158A mutant than in the wild type. Scholl et al. reported four additional families with FH-3 and a surprising genotype-phenotype correlation: two of the four families had a clinical course similar to that of the patients with the T158A mutation. Upon genetic testing, both families were found to have a germline mutation identical to one of the recurrent somatic *KCNJ5* mutations found in APAs (G151R). Of interest, the other two families had a germline mutation that affected the same amino acid but resulted in a glycine to glutamic acid substitution (G151E). This G151E mutation was more severe and associated with poorer survival than the other mutations. Scholl et al. suggested that the increase in Na⁺ conductance is responsible for cell death, which hinders the formation of adenoma and/or hyperplasia (Scholl UI et Al. 2012).

Germline mutations in *CACNAID* cause primary aldosteronism

After discovering *CACNAID* somatic mutations in APAs, Scholl et al. searched for *CACNAID* germline mutations in PA patients. They screened 100 unrelated patients with early onset PA and found two *de novo* mutations, which affected amino acids known to be target of somatic mutations in APA. The first subject had suffered from hypertension and heart disease since birth. Hypertension was refractory to treatment until amlodipine was used. The subject also exhibited seizures, cortical blindness, and neuromuscular abnormalities. He was found to harbour a p.Gly403Asp mutation in *CACNAID*. The second subject had cerebral palsy, spastic quadriplegia, mild athetosis, severe intellectual disability and seizures. By the age of 5 years, he displayed hypertension and hypokalemia. Genetic testing revealed a p.Ile770Met mutation in *CACNAID*. Because only two cases have been reported to date, definition of a phenotype for this association between germline *CACNAID* mutations and PA could be premature. Whether the clinical picture invariably affects many systems remains unclear.

Circulating-DNA:

A promising biomarker for early diagnosis of APA?

Circulating cell-free DNA

Cell-free fragments of DNA (cf-DNA) are extracellular nucleic acids that circulate freely into the bloodstream. Elevated levels of cf-DNA were first reported by Leon et al. in 1977 in the blood of patients with cancer. Since then, several studies confirmed the initial observation by Leon et al. (reviewed in Gormally et al), mostly in patients with breast and lung cancer (Chen XQ et al Nature Medicine 1996, Sánchez-Céspedes M et al 1998). Although the discovery of cf-DNA occurred more than seventy years ago, the source of cf-DNA remains still unclear and enigmatic. Several hypotheses were developed to explain the mechanisms of DNA release, but release from necrotic or apoptotic cells are the most accredited concept.

Cf-DNA can be considered as a photocopy of the cell that release it into the bloodstream. Therefore, it can give important information on genetic alterations, allelic imbalance and even presence of viral gene. For all these reasons, the fields of interest of cf-DNA as a predictive, diagnostic and non-invasive tool may be very numerous not restricted to oncology (Figure 12). Whether cf-DNA may allow detection of mutations is an emerging field of research.

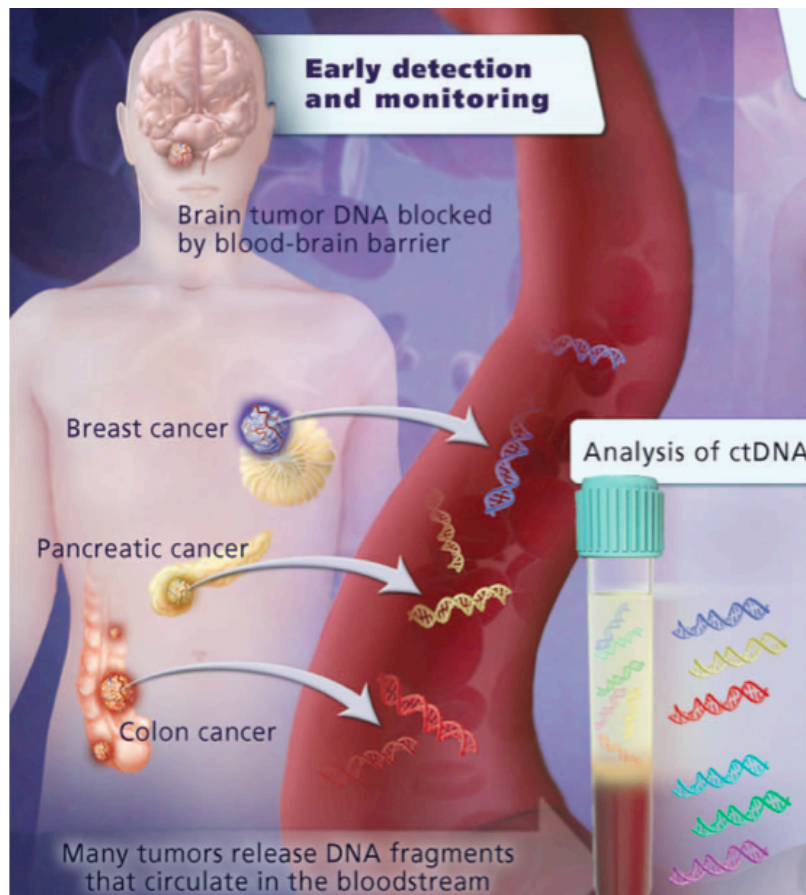


Figure 12: Potential applications of cf-DNA
(From Transl Med, 2014)

Origin of circulating-DNA: Cell Apoptosis and Necrosis

Apoptosis and necrosis are two distinct mechanisms of cell death and represent two extremes of the same phenomenon (DKanduc *et Al.* 2002). cf-DNA can be released from apoptotic or necrotic cells, reflecting a differential DNA origin, as well as from living cells through an active release (Van der Vaart M *et Al.* 2008, Chen Z *et Al.* 2005).

Tumor necrosis is a frequent event in solid malignant neoplasms, and it generates a spectrum of DNA fragments with different strand lengths because of random and incomplete digestion of genomic DNA by a variety of deoxyribonucleases. In general the length of these fragments of DNA is approximately 400–500 bp. However, in patients with cancer cf-DNA is released not only from necrotic cells, but also from cells undergoing apoptosis, autophagy, or mitotic catastrophe (Jin Z *et Al.* 2005).

Cell death in normal tissues occurs mostly via apoptosis that generates small and uniform DNA fragments usually from 185 to 200 bp in length (Giacona MB *et Al.* 1998; Chan KC *et Al.* 2008); this uniformly truncated DNA is produced by a programmed enzymatic cleavage process (Wyllie AH *et Al.* 1980).

Hence, cf-DNA is mainly released from apoptotic cells in healthy subjects whereas from necrotic cells in patients with cancer and, therefore, elevated levels of long DNA fragments could be used as marker of malignant tumor in blood. Recent studies showing increased levels of long cf-DNA in plasma from patients with breast (Umetani N *et Al.* 2006) and gynecologic cancers (Wang BG *et Al.* 2003) compared to the levels of healthy subjects, support this contention. (Sabine Jahret *et Al.* 2001).

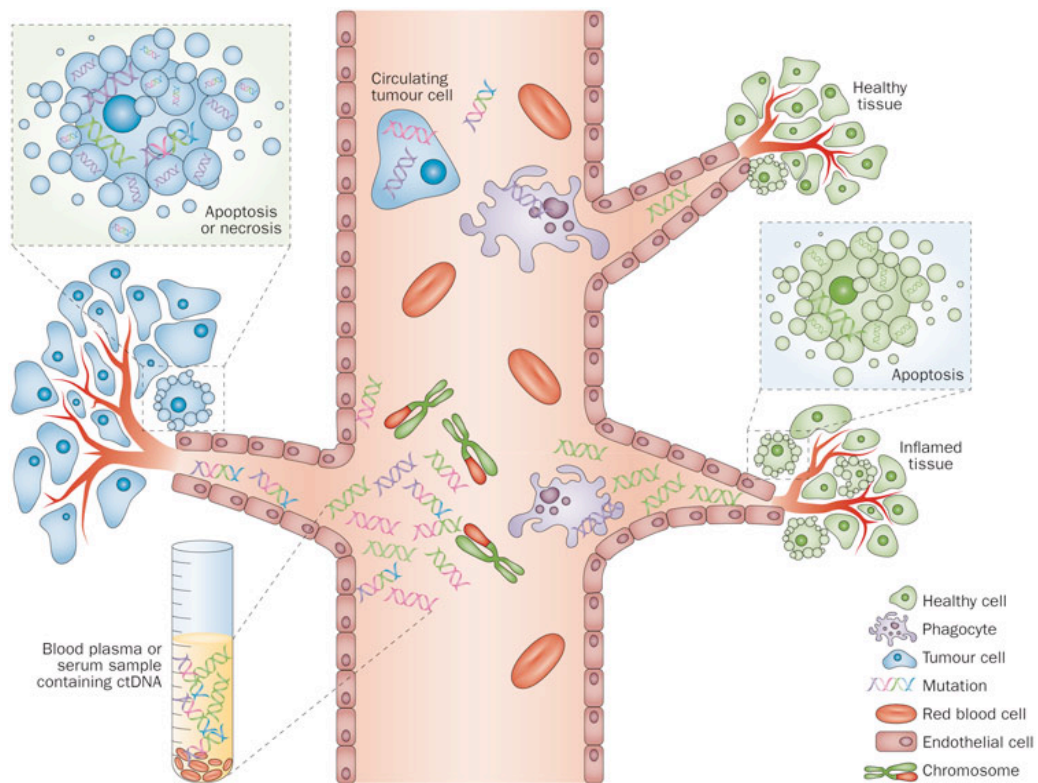


Figure 13: Different Mechanisms of release of cell- free DNA in bloodstream (Nature 2013)

Since the length of cf-DNA reflects the mechanisms, apoptosis or necrosis, by which DNA fragments are generated (Figure 13), the ratio of longer-to-shorter fragment concentration, also known as fragmentation index (DII), can be assumed as measurement of DNA integrity.

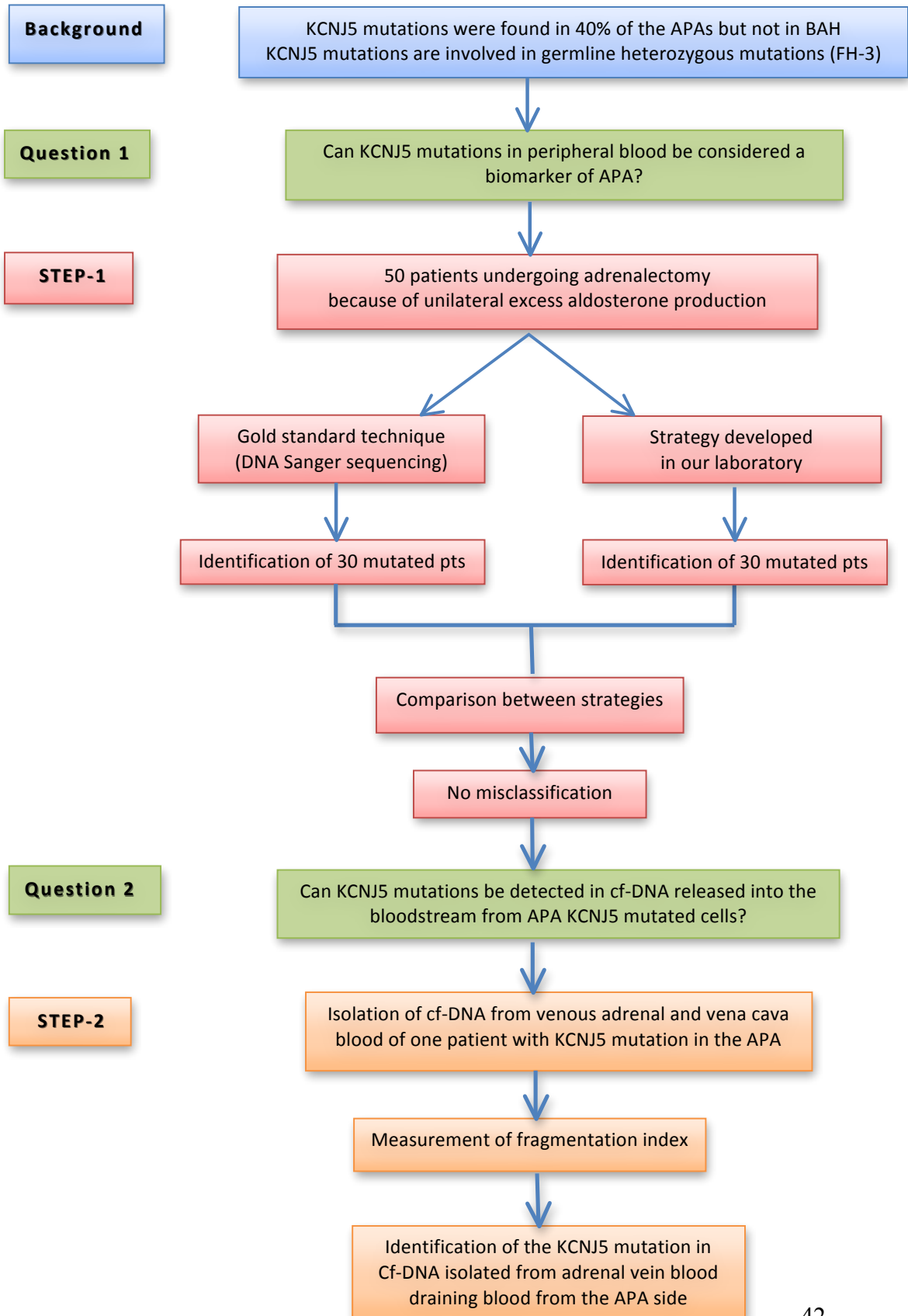
Aims

The general aim of our study was to test the hypothesis that DNA released into bloodstream from the APA cells that harbour a KCNJ5 mutation (mutated) also contains the KCNJ5 mutation. Because the contralateral adrenal gland (wild type) contains no mutation, detection of KCNJ5 mutation in the adrenal venous blood would be much easier from the APA side.

Specific aims:

1. To develop an accurate but less time consuming method than Sanger sequencing to pinpoint KCNJ5 mutations in the APA tissue.
2. To isolate cf-DNA from the adrenal veins and inferior vena cava in the patients undergoing AVS.
3. To evaluate if this method could be also used to identify KCNJ5 mutations in cf-DNA isolated from the adrenal vein blood draining the APA with known KCNJ5 mutations.
4. To investigate the fragmentation level of cf-DNA. Different levels of fragmentation may be suggestive of apoptosis or necrosis and, therefore, fragmentation could provide information on the mechanisms by which cf-DNA is released from APA cells.

Flow-chart of the study



Materials and Methods

DNA Extraction from APA tissue

The adrenal gland tissue was obtained from PA patients with lateralized excess production of aldosterone undergoing adrenalectomy. The tissue was collected under sterile conditions in the operating room after cutting the gland into halves. Half of the adrenal was sent to the pathology department for histology and the remaining tissue was used for downstream analysis. The diagnosis of APA was confirmed at histopathology and moreover, all patients displayed normokalemia and improvement in blood pressure control at postoperative follow-up. Hence, all *four corner criteria* were satisfied in each patient.

DNA was isolated from 40 mg of tissue previously cut in small pieces (about 3-4 mm³) using Euro Gold Tissue-DNA Mini Kit according to manufacture instructions. Elution final volume was 100 ul. Evaluation of the concentration and purity of DNA as a ratio of absorbance at 260 nm and 280A (ratio of ~1.8 is generally accepted as “pure” for DNA) was assessed with Thermo Scientific Nano Drop 2000 spectrophotometer.

Taq-Man probe

Three different couples of primers for KCNJ5 gene were drawn to evaluate the presence of mutation in the DNA extracted from tissue of APA patients. In particular, two couples of primers recognized the most frequent mutated regions that include G151R and L168. Both primers produced 200 bp amplicons. The third couple of primers generated a 400 bp product of PCR that covers both mutations (G151R and L168R).

Five different Taq-man hydrolysis probes were designed to increase the specificity of quantitative PCR thanks to the perfect binding of oligonucleotides that recognize both wild type and mutated regions. A Taq-man probe consists of two types of fluorophores, which are the fluorescent parts of reporter proteins. While the probe is attached to the DNA template and before the polymerase acts, the quencher (Q) fluorophore reduces the fluorescence of the reporter (R) fluorophore.

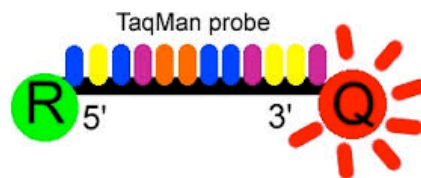


Figure 14: Scheme of a Taq-Man probe

During the PCR reaction, exonuclease activity of *Taq*- polymerase cleaves a dual-labeled probe during hybridization to the complementary target sequence and this allows the separation of the quencher from the reporter that is able to issue the fluorescence.

Hence, fluorescence detected in the quantitative PCR thermal cyclers is directly proportional to the fluorophore released and also to the amount of DNA template generated during PCR reaction.

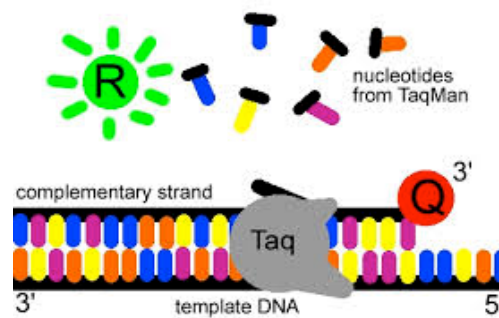


Figure 15: Release of reporter by Polymerase and emission of fluorescence during Q-PCR

We used the following fluorophores for TAQ-MAN probes:

1. 5'FAM, 3'BHQ1 for wild type region of G151R
2. 5'Texas Red, 5'HEX 3'BHQ1 for mutated regions of G151R
3. 5'FAM, 3'BHQ1 for wild type region of L168R
4. 5'Texas Red, 5'HEX 3'BHQ1 for mutated region of L168R

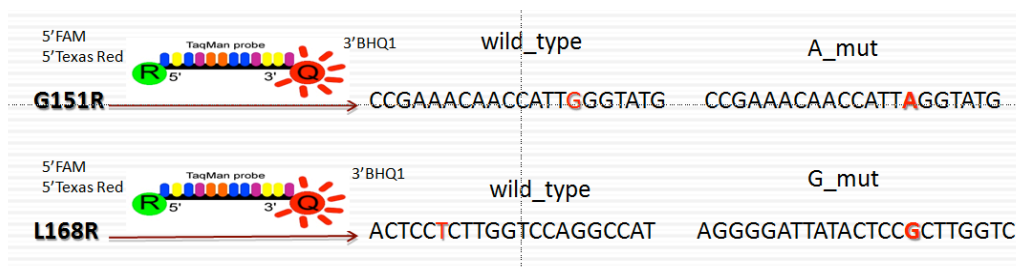


Figure 16: Design of Taq-man Probe

Gradient curve

Before performing Q-PCR, a gradient curve was done to verify the best annealing temperature (T_a) of the primers. Melting curves were obtained by increasing the temperature from 65°C to 95°C with a plate that was read every 0.3°C after holding the temperature for 5 sec. For G151R and L168R the gradient curve was performed from 65°C to 55°C.

Real time PCR (Q-PCR)

CFX96 Touch Real-Time PCR machine (Bio-Rad) was used to perform the reactions of Real Time PCR (Q-PCR) for KCNJ5 gene. Q-PCR amplifications were carried out in a reaction final volume of 25 ul. Each PCR reaction mixture was composed of 12.5 ul of PCR mix (SsoFast™ Eva Green® Super mix Bio-Rad) 1.5 ul of each primer (300nm/ul) 4.5 ul of water and 5 ul of DNA extract. Every reaction was carried in duplicate. Thermal cycling was organized in 3 repeated steps: a first denaturation step of 3 min at 95°C, followed by 40 repeated cycles of 95°C for 10 sec and 60°C for 30 sec. Q-PCR amplifications with Taq Man Probe were carried out in a reaction final volume of 15 ul. Each PCR reaction mixture was composed of 10.8 ul of PCR mix (Sso Advanced universal Probes supermix Bio-Rad, Berkeley California) 1.2 ul of each primer (300nm/ul) and 0.45 ul of probes (300nm/ul).

Thermal cycling conditions included the following 3 steps: denaturation of 3 min at 95°C, followed by 40 repeated cycles of 95°C for 10 sec, and finally 55°C for 30 sec. To verify the presence of the mutation the three probes were loaded in same well of PCR plates. Two amplification curves were obtained, one corresponding to the wild type and the other one to the mutated region.

Allelic discrimination by Genotype Assignments

Assignment of genotypes to wild type or mutant, i.e. allelic discrimination, was based on the analysis of the amplification plots generated for each allele-specific TAQ-MAN probe (FAM, Texas Red, and HEX). Allelic discrimination analysis was performed using a module included in the software package of CFX96 I Cyclor IQ Touch Real-Time PCR machine (Bio-Rad Hercules, United States).

After assigning genotypes, the software packages analyze either the final relative fluorescent units (RFU) or the C_t values and reported graphs data as scatter plot. In this way, the genotypes assigned to each gene were plotted, thereby allowing discrimination between alleles.

Sanger Sequencing

Sanger sequencing was performed to confirm the results obtained with Q-PCR using the Taq Man probes. The PCR product was purified with QIAquick PCR Purification Kit according to manufacture instructions (Qiagen, Hilden, Germany) and eluted to 40 ul final volume. The PCR purified product (25 ul + 5 ul of Gel Loading Buffer with DNA Stain (Jena Bioscience) was loaded on 2% Agarose gel (2 gr of Agarose dissolved in 100 ml 1X TAE buffer) to verify the absence of primer-dimers.

The quantity of PCR product was measured with Thermo Scientific Nano Drop 2000 spectrophotometer. The sample was opportunely diluted, dried for 15-20 minutes and sent to BMR Genomics (spin-off of the University of Padua) where Sanger Sequencing was performed.

Collection of human plasma from adrenal veins and inferior cava

Adrenal Vein Sampling (AVS) is currently performed at our centre by an interdisciplinary team with extensive expertise in this field. After an hour of supine rest of the patient and correction of hypokalaemia, if present, blood was obtained from the two adrenal veins (right and left side) and inferior vena cava. Blood samples were collected in EDTA tubes and kept at 4C until measurements of cortisol and aldosterone. The cannulation was considered successful when selectivity index (Cortisol adrenal vein/ Cortisol inferior adrenal vein) was ≥ 1.1 ; lateralization index ≥ 2 ([A / C] adrenal vein / [A / C] adrenal vein contralateral) indicated lateralized excess aldosterone production (Rossi GP et Al 2001).

Circulating DNA (ct-DNA) extraction from plasma of APA patients

Blood obtained from the adrenal veins and inferior vena cava was first centrifuged at 3300 RPM for 15 minutes at 4C and then centrifuged again at 16,000 RPM for 10 minutes at 4 C to remove cellular debris. Ct-DNA was extracted from 1ml of plasma using Qiamp DNA blood mini kit (Qiagen, Hilden, Germany) according to manufacture instructions. Cf-DNA was eluted in 30 ul of elution buffer.

Plasma DNA concentration and integrity index

Since ct-DNA levels were too low to be measured with Nano drop 2000 spectrophotometer we used a PCR based approach for ct-DNA measurement.

Genomic DNA ranging from 10 ng/ul to 0.0016 ng/ul dilutions was used to build a PCR standard curve. The absolute concentration of ct-DNA was calculated using the standard curve.

The same curve was also used to calculate the integrity index (DII), defined as ratio of longer (400 bp) to shorter amplicons (200bp) generated at the end of Q-PCR. $DII \geq 1.0$ was assumed to denote cf-DNA integrity. The specific primers to perform such Q-PCR are reported in Figure 17.

Gene	Amplicon lengths	Forward primer	Reverse primer
KCNJ5 (G151R, L168R)	400 bp	TCAGGTTGACGCCGCTGT	GAGAGATAGAATACATTACTGATGTGTGGAT
KCNJ5 G151R	200 bp	TCAGGTTGACGCCGCTGT	TTCGTAGCCGTTCTGCTGC
KCNJ5 L168R	200 bp	TCAGGTTGACGCCGCTGT	TCTATAAATGGACACCGATGGGTAGT

Figure 17: Primer design

High resolution melting analysis (HRM)

High resolution melting analysis (HRM) is a powerful technique that allows detection of mutations, polymorphisms and epigenetic differences in double-stranded DNA samples. HRM provides post-PCR analysis that characterizes DNA samples on the basis of the dissociative behavior (dsDNA-ssDNA) with increasing temperature. The classic Q-PCR is first necessary to amplify the DNA region in which the mutation of interest takes place. Once PCR has ended, HRM analysis can begin.

HRM process simply consists in a precise warming of the DNA amplicon from around 50°C up to around 95°C (an increase of 0.2 °C or 0.3 °C per seconds is usually used). At some point during this process, the melting temperature of the amplicon is reached and the two DNA strands separate or “melt” apart. The melting curve is produced by measuring the fluorescence of the amplification in relation to the temperature increase. The fluorescence values decrease with increasing temperature (dsDNA to ssDNA). To view the T_m , the negative derivative of the temperature is plotted in the pre-melt region where the values of fluorescence are 100% because the DNA is double stranded. Data analysis allows identification of homozygous and heterozygous samples and discrimination into different clusters. Hence, HRM can be considered one the most relevant next-generation PCR applications.

High resolution melting assays require a real-time PCR detection system with excellent thermal stability and HRM-dedicated software. HRM analysis was performed in our laboratory using CFX96 Touch Real-Time PCR machine additioned with specific software for Processing Melt Curve Data. This software allows a quick analysis of the data sets obtained from PCR and identification of DNA sequences based on their composition, length, GC content and strand complementarity.

Protocol for PCR and HRM analysis

PCR amplifications were carried out in a reaction final volume of 10 ul. Each PCR reaction mixture was composed of 6.25 ul of PCR mix (SsoFast™ Eva Green® Super mix) 0.75 ul of each primers (300nm/ul) 2.25 ul of DNA with final concentration of 2ng/ul. Melting curves were obtained by increasing the temperature from 65 °C to 95°C with a ramping of 0.3 °C for 10 seconds for L168R region and 0.3°C for 5 seconds for G151R. This approach was used to evaluate the different melting temperature (T_m) of wild type and mutated heteroduplexes of circulating DNA that are generated at the end of Q-PCR to pinpoint the difference between the different clusters generated from normalized melting curves. Wild type and mutated tissue of the corresponding plasma patients were used as controls.

Statistical Analysis

Results about concentrations of cf-DNA were expressed as mean. Integrity Index differences between groups were analyzed by t-test and, for multiple group comparison, by one-way ANOVA. The differences were considered to be significant at $p < 0.05$. Statistical analyses were performed using Graph pad/prism 5 for Windows software (Graph pad Software, La Jolla, California, USA; www.graphpad.com).

Results

Identification of KCNJ5 mutations in the APA tissue with Taq-man probe based technique

We first assessed the specificity of TAQ-MAN probes designed to detect L168R and G151R mutations in KCNJ5 gene by performing a gradient curve from 66°C to 55°C. This step is preliminary to Q-PCR and fundamental to evaluate the best annealing temperature (T_a) of the primer and the probe during the Q-PCR reaction. The reporter probes HEX and TEXAS RED were used for L168R and G151R regions, whereas FAM was used for wild type one. Because a synonymous mutation characterized by substitution of A with C was found for G151R mutation, we designed an additional probe that covers this mutated region.

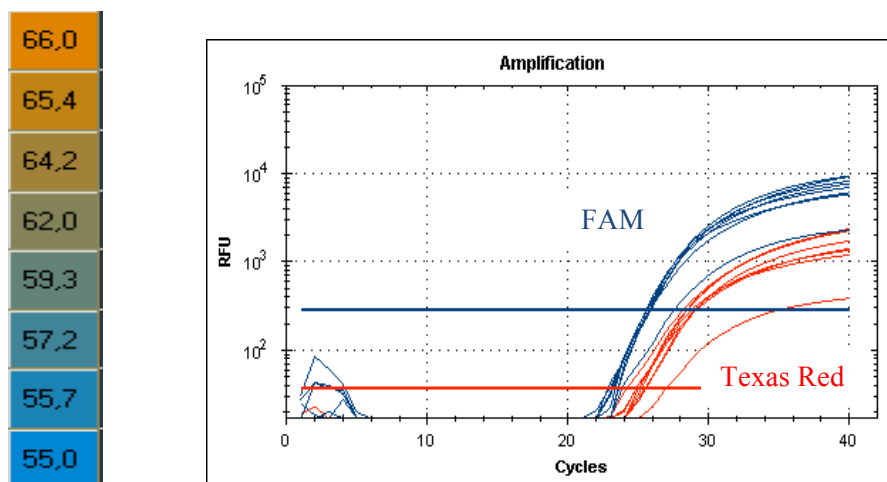


Figure 18: Amplification curve in Q-PCR for L168R mutated region (T/G)

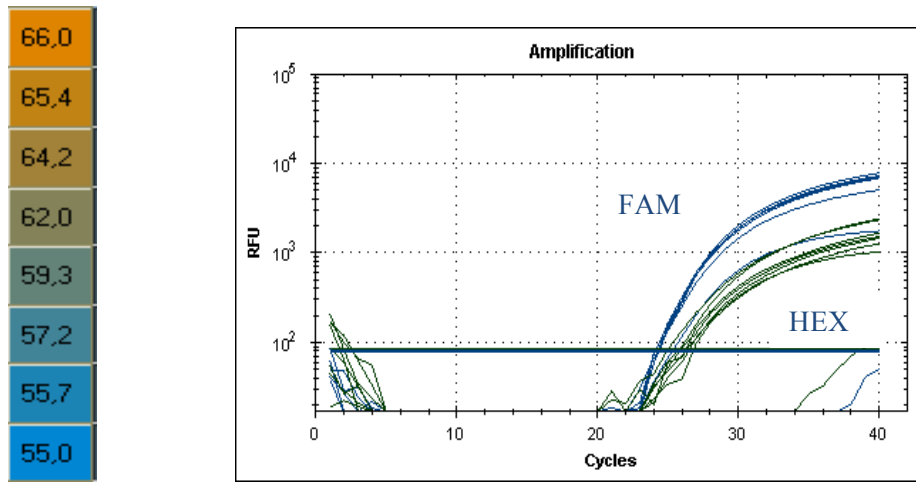


Figure 19: Amplification curve in Q-PCR L168R mutated region (T/G)

We found that the annealing temperatures for the best discrimination of L168 mutated region are: 62.0°C for FAM/TEXAS RED and 59.3°C for FAM/HEX (Figures 18 and 19). The annealing temperatures for the best discrimination of G151R mutated region are: 57.0°C for FAM/TEXAS RED and 62.0°C for FAM/HEX (Figures 18 and 19).

66.0
65.4
64.2
62.0
59.3
57.2
55.7
55.0

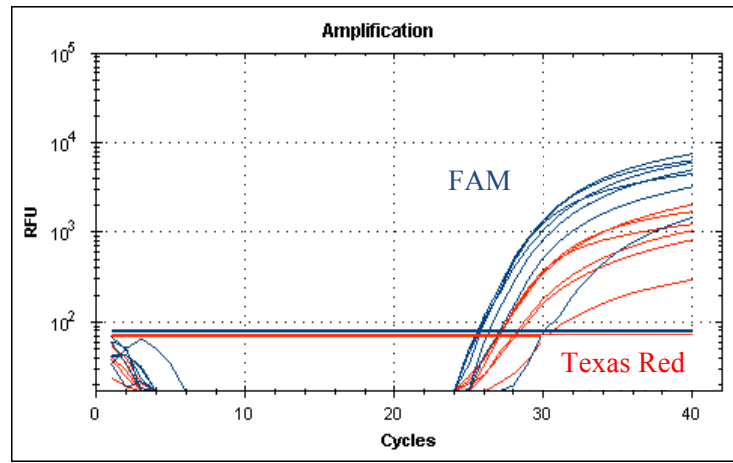


Figure 20: Amplification curve in Q-PCR G151R mutated region (A/G)

66.0
65.4
64.2
62.0
59.3
57.2
55.7
55.0

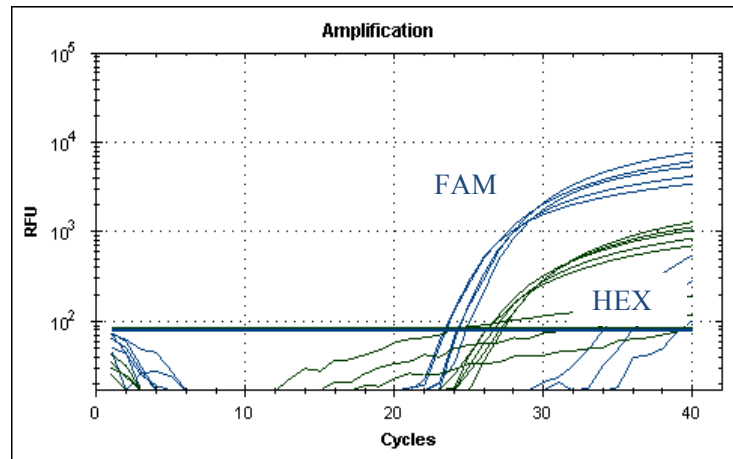


Figure 21: Amplification curve in Q-PCR G151R mutated region (A/G)

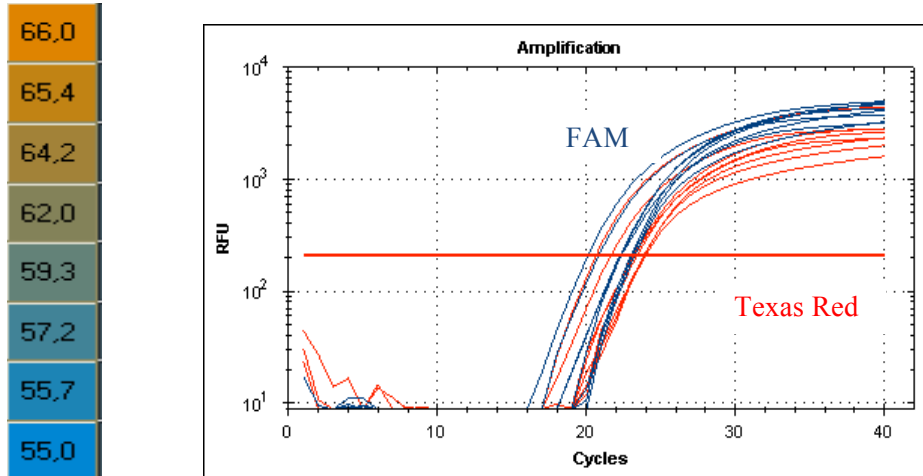


Figure 22: Amplification curve in Q-PCR G151R mutated region(C/G)

The best annealing temperatures for the synonymous mutation were 59.4°C and 60.0°C (Figure 22). After establishing that each probe can discriminate between mutation and wild type, an additional experiment was performed to evaluate if the two probes designed for G151R mutated region interfere between them. For this experiment, both mutated probes (A/G, C/G) were loaded in the same well.

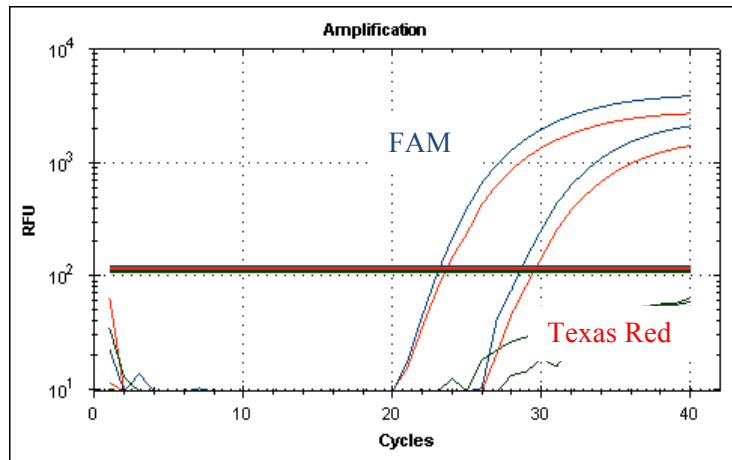


Figure 23: Amplification curve in Q-PCR G151R mutated region (C/A)

Fluor	Content	Sample	C(t)
FAM	Pos Ctrl		28,63
FAM	Pos Ctrl		23,13
HEX	Pos Ctrl		N/A
HEX	Pos Ctrl		N/A
Texas Red	Pos Ctrl		29,51
Texas Red	Pos Ctrl		23,56

Figure 24: Threshold cycle (Ct) of amplification

In a sample with synonymous mutation, the lack of interference between the probes was demonstrated by the amplification of only Texas Red, i.e. the probe that recognized base C. No amplification was observed for HEX.

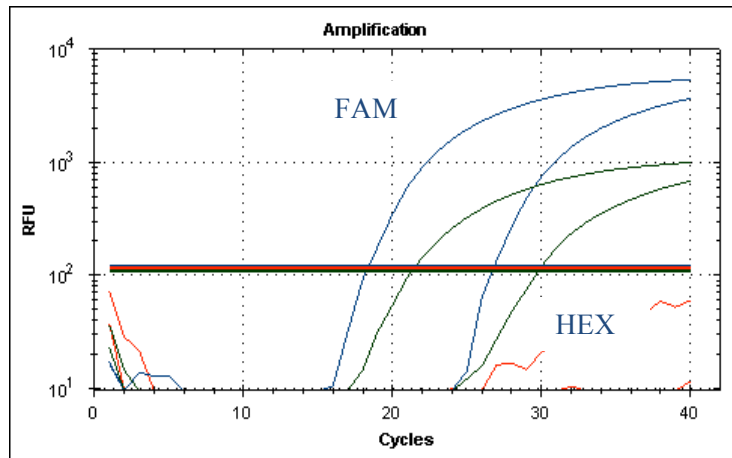


Figure 25 Amplification curve in Q-PCR G151R mutated region (A/C)

Fluor	Content	Sample	C(t)
FAM	Pos Ctrl		18,32
FAM	Pos Ctrl		26,77
HEX	Pos Ctrl		21,25
HEX	Pos Ctrl		29,74
Texas Red	Pos Ctrl		N/A
Texas Red	Pos Ctrl		N/A

Figure 26: Threshold cycle (C_t) of amplification curve

For mutated Taq-Man probe in HEX that recognized base A instead than C, the result in Figure 26 shows no amplification for TEXAS RED as expected.

Allelic discrimination

At the end of entire cycle of Q-PCR with TAQMAN probes, genotypes are assigned by analyzing the amplification plots generated for each allele-specific, as described in detail in Material and Methods. The heterozygote population was showed with triangle and the WT population with red circle. These results show the clear difference about the two examined populations, with the first plot for G151R wild type and the mutated one (Figure 27) and the second one for L168R (Figure 28).

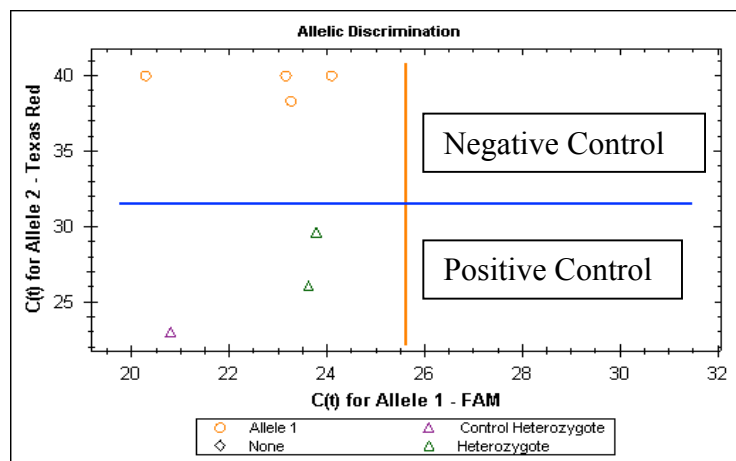


Figure 27: Allelic discrimination on for G151R

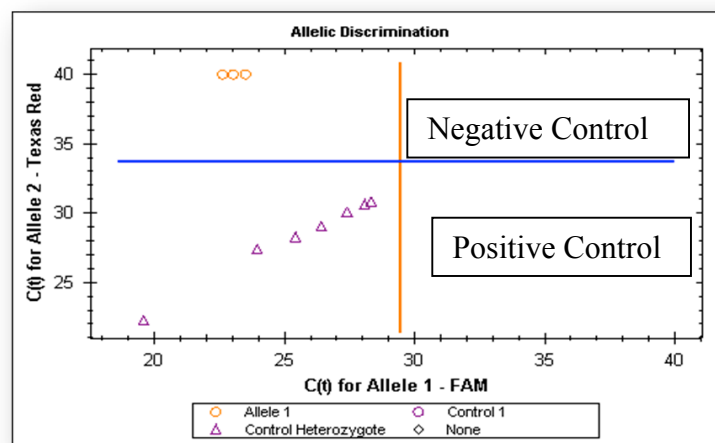
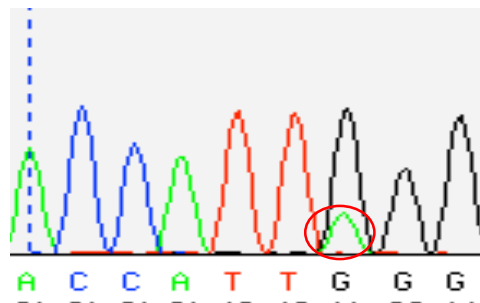


Figure 28: Allelic discrimination for L168R

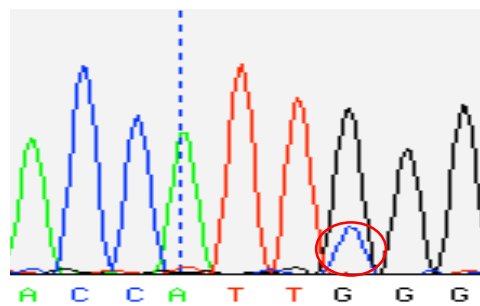
Validation of new Taq--man based technique with Sanger Sequencing

The results obtained with Taq-man probe were compared to those obtained with Sanger sequencing used as the gold standard method (Figure 29). Each mutation found with Taq-Man probes was detected with Sanger, and all mutations revealed with Sanger were found with Taq-man probes. Hence, these results showed high specificity and sensitivity of the probes designed in our laboratory and then suggests that they could be used for detecting KCNJ5 mutations.

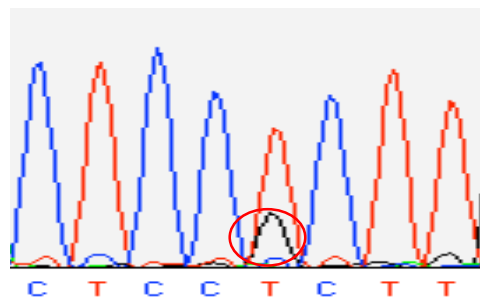
Figure 29



G151R A/G



Synonymous mutation G151R C/G



L168R G/T

Cell-free DNA isolation from plasma of Adrenal Vein Sampling

In order to test the hypothesis that KCNJ5 gene mutations can be detected in cell-free nucleic acids that are released in the adrenal vein blood, we first evaluated the feasibility of isolating cf-DNA from AVS plasma. Then, we quantified cf-DNA and evaluated fragmentation index to investigate the mechanism (apoptosis or necrosis) by which cf-DNA is released from APA cells. Finally, we applied the Taq-man probe based technique to cf-DNA to detect KCNJ5 mutations.

The first step was identification of the best operative procedure to isolate cf-DNA (Figure 30).

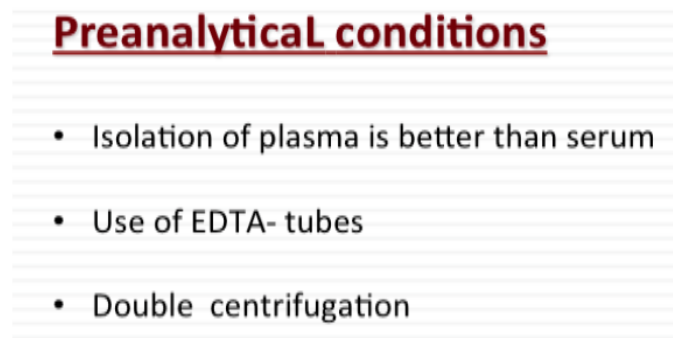
- 
- Preanalytical conditions**
- Isolation of plasma is better than serum
 - Use of EDTA- tubes
 - Double centrifugation

Figure 30: Preanalytical conditions

To identify the starting volume of plasma needed to isolate cf-DNA, various amounts of plasma volume, ranging from 250 ul to 1000 ul, were used. Figure 31 shows 2% agarose gel where four different Q-PCR products of KCNJ5 gene expression were loaded. We obtained the best result from 1 ml plasma, as shown in lane 1.

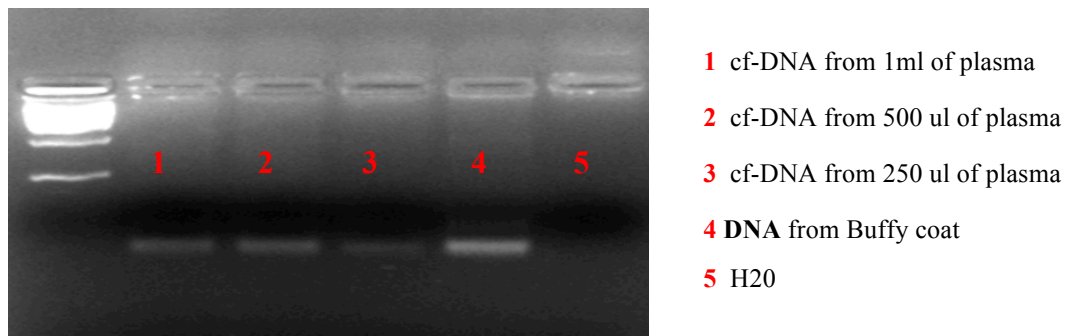


Figure 31: 2% Agarose gel with cf-DNA extracted from different amounts of plasma

Calibration line for quantification of G151R 200pb fragment

After confirming the expression of KCNJ5 gene in cf-DNA extracted from plasma obtained during AVS sample and verifying the product of PCR on agarose gel, we measured the concentration of cf-DNA with Q-PCR absolute quantification. Figure 32 shows the amplification curve for G151R region that produces amplicon of 200 bp, whereas the calibration line and the C_t value for each standard (corresponding to known concentrations of genomic DNA extracted from buffy coat) are shown in Figure 34. The dilutions were made from 10 ng/ul to 0.016 ng/ul. All samples were loaded in duplicate.

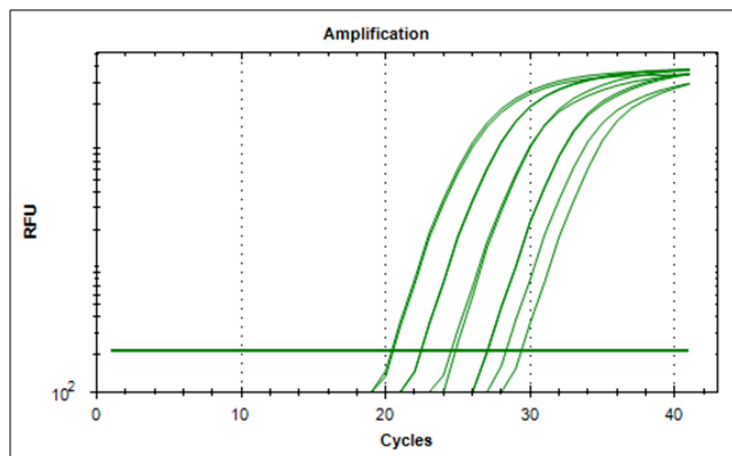


Figure 32: Amplification Curve of diluted genomic DNA from 10 to 0.016 ng/ul

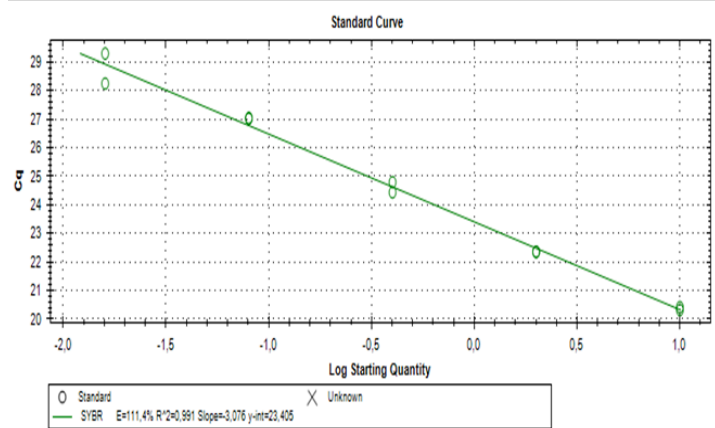


Figure 33: Calibration line of diluted genomic DNA from 10 to 0.016 10ng/ul

Std-01	20,42
Std-01	20,32
Std-02	22,35
Std-02	22,36
Std-03	24,79
Std-03	24,44
Std-04	27,05
Std-04	27,02
Std-05	28,25
Std-05	29,30

Figure 34: Ct value of standard dilution from 10ng/ul to 0.016 of genomic DNA

Calibration line for quantification of L168R 200 bp fragment

Similar experiments were made for L168R 200 bp fragments. Below are reported the amplification curve for L168R region that produces 200 bp amplicon (Figure 35), the calibration line (Figure 36) and the value of C_t of each standard corresponding to genomic DNA extracted from buffy coat. The dilutions are made from 10 ng/ul to 0.016 ng/ul. All samples were loaded in duplicate.

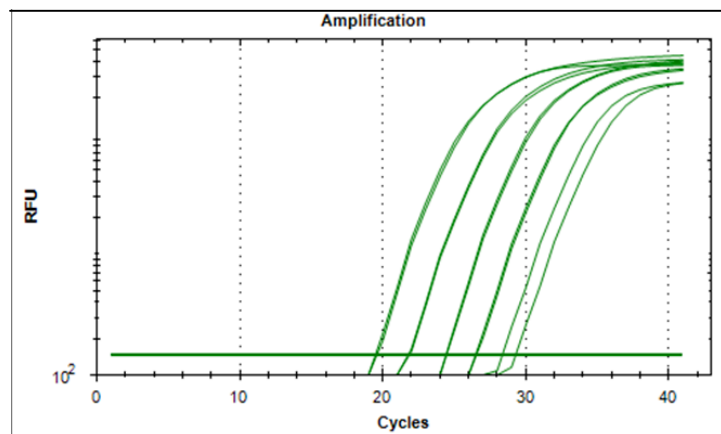


Figure 35: Amplification Curve of diluted genomic DNA from 10 to 0.016 ng/ul

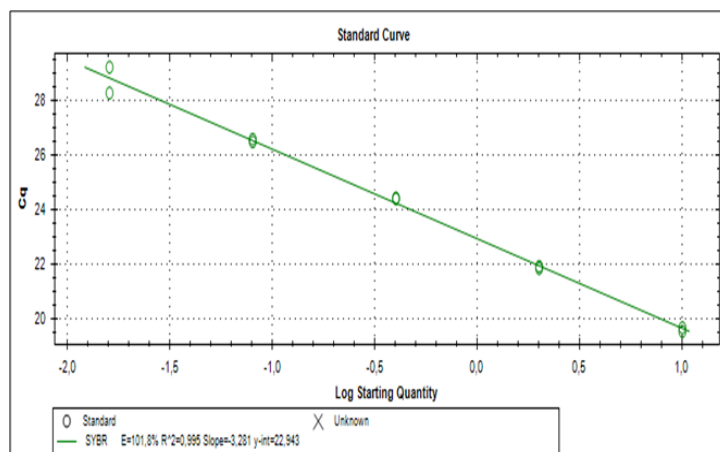


Figure 36: Calibration line of diluted genomic DNA from 10 to 0.016 10ng/ul

Std-01	19,69
Std-01	19,55
Std-02	21,93
Std-02	21,86
Std-03	24,41
Std-03	24,44
Std-04	26,59
Std-04	26,50
Std-05	28,23
Std-05	29,29

Figure 37: C_t value of diluted standard genomic DNA (Std) from 10 to 0.016 ng/ul

Calibration line for quantification of 400 bp fragment

Similar Experiments were similarly made for 400 bp fragment, using the dilutions from 10 ng/ul to 0.016 ng/ul and loading the samples in duplicate.

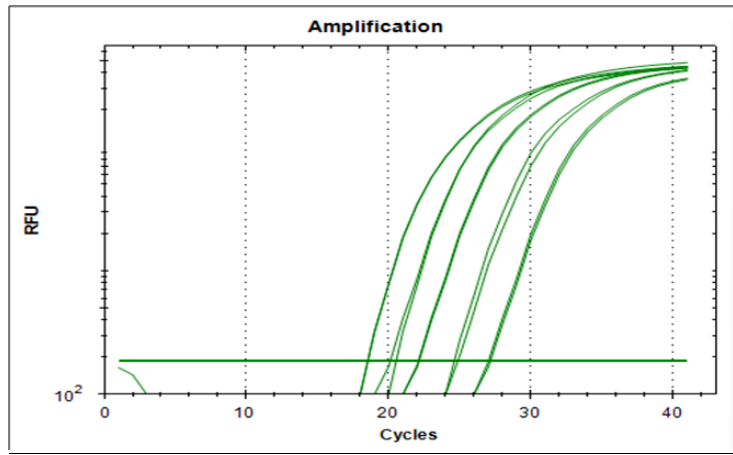


Figure 38: Amplification Curve of diluted genomic DNA from 10 to 0.016 ng/ul

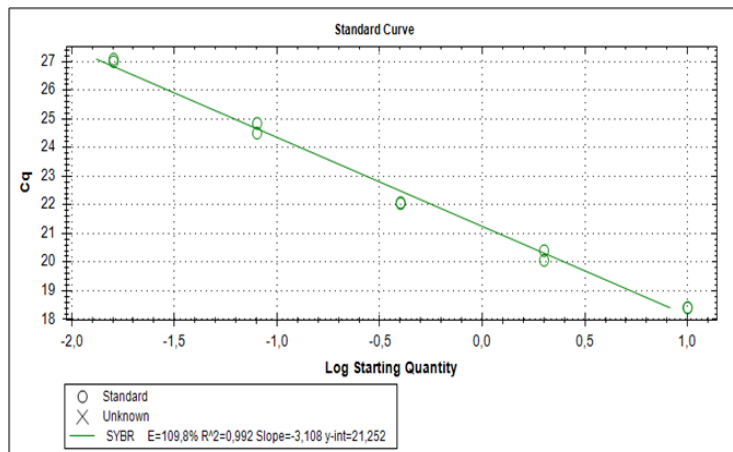


Figure 39: Calibration line of diluted genomic DNA from 10 to 0.016 10ng/ul

Std-1	18,41
Std-1	18,41
Std-2	20,40
Std-2	20,07
Std-3	22,08
Std-3	22,05
Std-4	24,51
Std-4	24,85
Std-5	27,09
Std-5	27,00

Figure 40: C_t value of diluted standard genomic DNA (Std) from 10 to 0.016 ng/ul

Absolute quantification of circulating DNA

We calculated the absolute concentration of cf-DNAs extracted from inferior vena cava, right and left adrenal vein plasma collected during AVS. Plasma from peripheral blood of the patients undergoing AVS and plasma isolated from patients suffering with stomach cancer were used as positive controls. The table (Figure 41) below shows the absolute concentration values for each sample expressed as mean (ng/ul).

<u>Cf-DNA</u>	<u>Number of patients</u>	<u>Concentration mean ng/ul</u>
<u>Stomach cancer</u>	<u>3</u>	<u>7.15</u>
<u>Peripheral blood</u>	<u>12</u>	<u>0.68</u>
<u>Left Plasma (L)</u>	<u>12</u>	<u>0.46</u>
<u>Right plasma (R)</u>	<u>12</u>	<u>0.37</u>
<u>Cava Vein</u>	<u>12</u>	<u>0.76</u>

Figure 41: Concentration values of cf-DNA

Evaluation of fragmentation through Integrity index

The integrity index was calculated as reported in detail in Material and Methods, starting from the concentration of each amplicon generates at the end of Q-PCR. In particular each integrity index (DII) was calculated as the ratio of longer (400bp) to shorter amplicons (200bp). In the bar graph below (Figure 42) are reported the results obtained from the samples whose concentrations are shown in Figure 41. DII was significantly lower in AVS than in cancer patients; thereby suggesting that apoptosis is the prevalent mechanism by which cf-DNA is released from the APA cells.

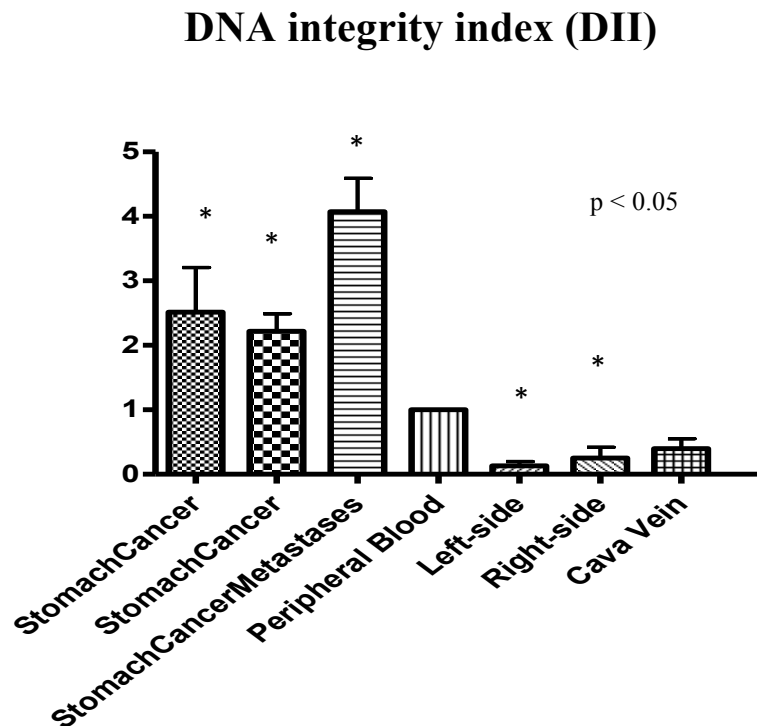


Figure 42: The bar graph shows that DNA integrity index (DII) is higher for cf-DNA isolated from blood of stomach cancer patients than DII of blood peripheral plasma, adrenal veins and inferior vena cava of APA patients. The major length of cf-DNA released from stomach cancer patients could be related to necrosis events that are less evident in APA patients.

HRM analyses of DNA from APA tissue

After measuring the length of ct-DNA isolated from AVS plasma and understanding that such ct-DNA could derive from apoptotic cells released from APA tissue, we evaluated the feasibility of pinpointing the mutations in KCNJ5 gene using ct-DNA. We focused our attention on cf-DNA because AVS procedure is quite invasive and, therefore, the possibility of identifying gene mutations with cf-DNA seemed very attractive.

To pursue this aim we exploited HRM-based technique that discriminates wild type and mutated heteroduplexes generated during the Q-PCR by analyzing melting temperature (T_m). At that temperature the strands of double DNA helix are separated, and heteroduplexes can be detected because of their specific denaturation melting temperature.

The figures below show the results obtained from HRM for G151R mutation. To assess the best operative conditions, cf-DNA obtained from APA tissue was serially diluted (from 10 ng/ul to 0.016 ng/ul) to assess the sensitivity of HRM analyses (Figure 38). Correct dilution and purity of the sample are essential conditions to obtain optimal results from HRM. Figure 43 shows the melting peak for G151R mutation, whereas Figures 44 and 45 show the differences between normalized melting curves of mutated and wild type tissues, and the differences between different clusters within membership (Figure 42).

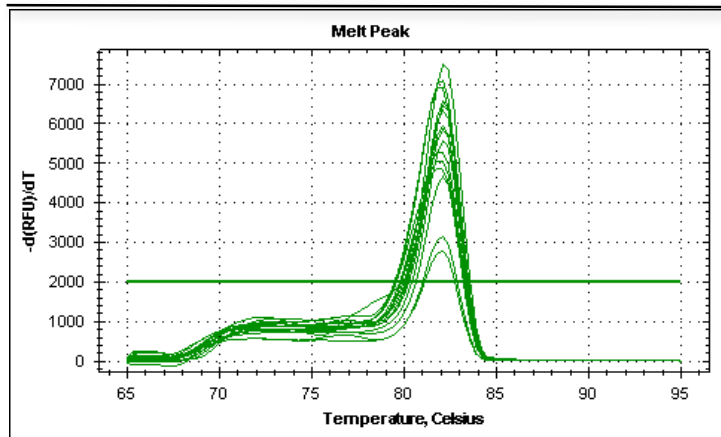
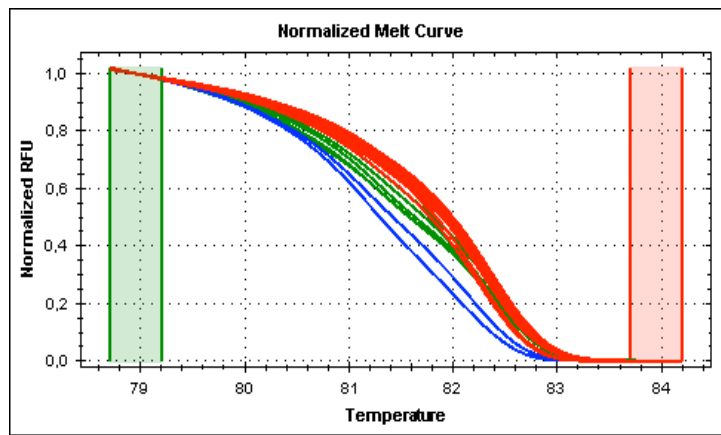
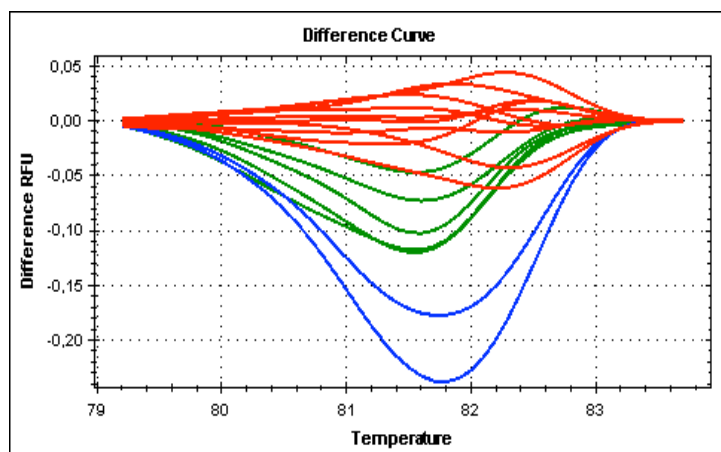


Figure 43: Melting peak of G151R



DNA from mutated tissue in C
 DNA from wild type
 DNA from mutated tissue in A

Figure 44: Normalized G151R melting curve



DNA from mutated tissue in C
 DNA from wild type
 DNA from mutated tissue in A

Figure 45: Normalized G151R melting curves give different clusters

HRM analyses of circulating DNA from AVS sample

After establishing that KCNJ5 mutations can be detected even using a very low concentration (0.4 ng/ul) of DNA, we isolated cf-DNA from the adrenal veins of a patient with somatic L168R mutation in the APA located in the left adrenal gland.

The first step was performing a gradient curve to identify the best annealing temperature of primers for L168R region. The best results in terms of amplification were obtained with an annealing temperature of 53.0°C and 54.9°C. HRM analysis for L168R region was performed with 54.9°C annealing temperature and increasing temperature for melting analysis from 65°C to 95°C with ramping of 0.3°C for 10 seconds. Under these conditions we discriminated wild type from mutated circulating DNA. The same results were obtained from three different experiments.

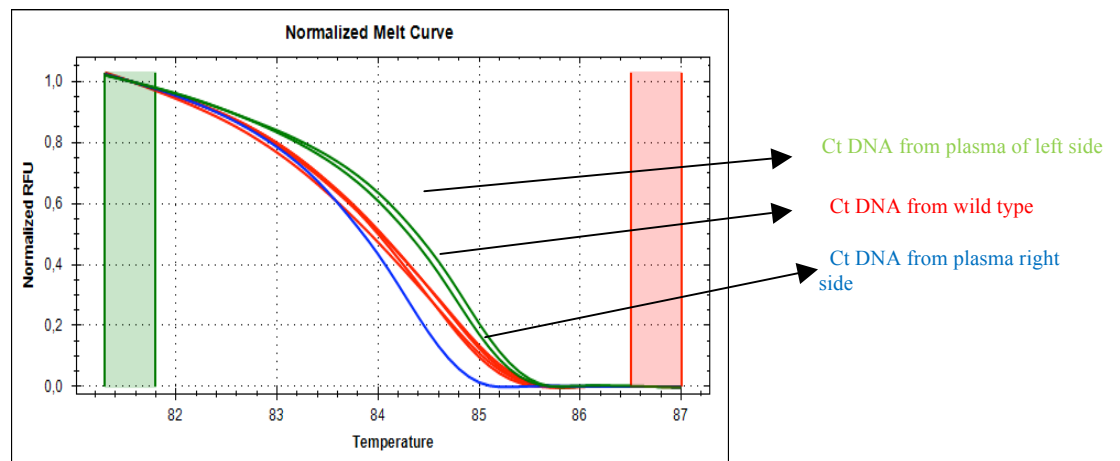


Figure 46: Normalized L168R melting curve

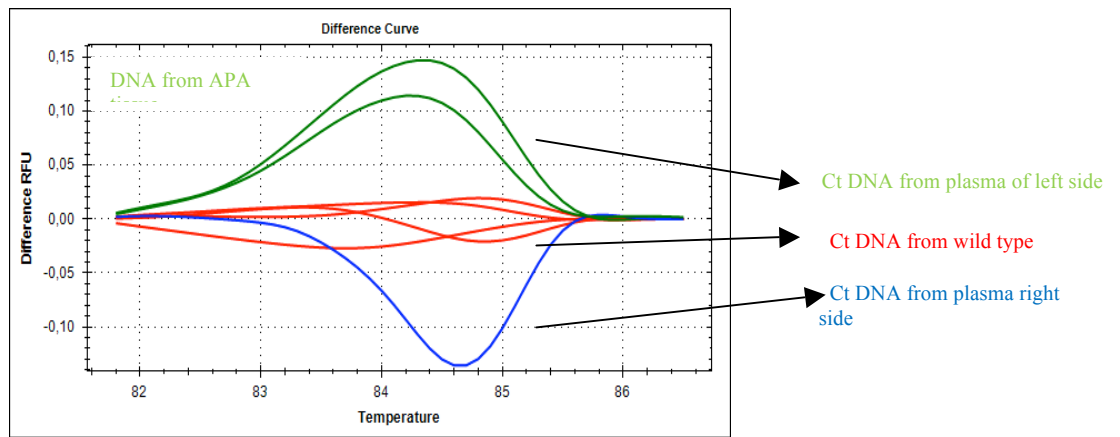


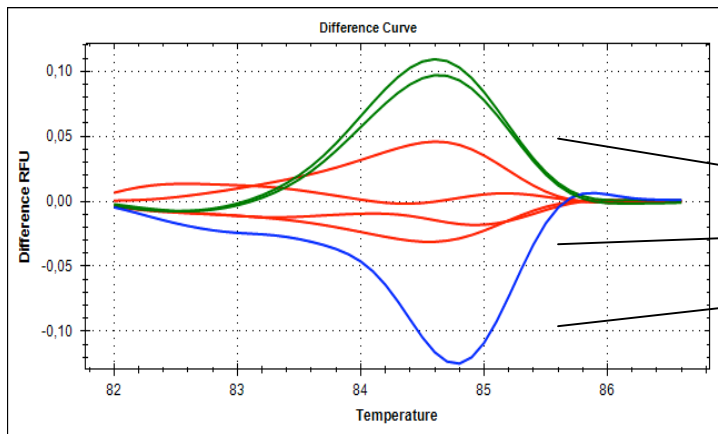
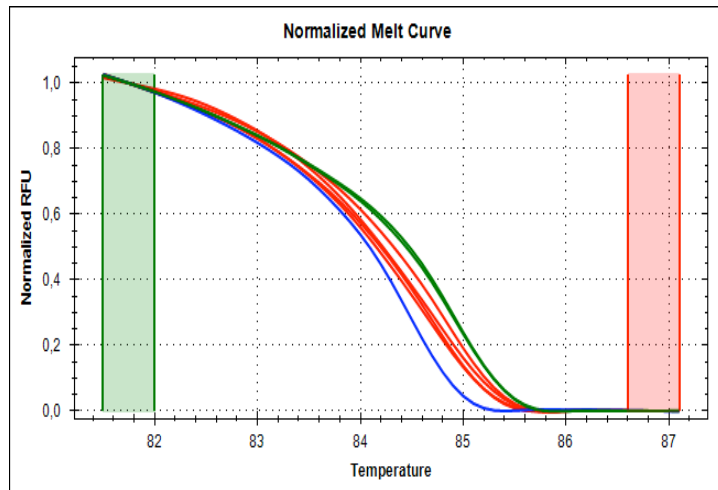
Figure 47: Normalized melting curves give different L168R clusters

Sample	Cluster	Percent Confidence
	Cluster 1	98.7
	Cluster 1	99.2
	Cluster 1	99.2
	Cluster 1	96.5
	Cluster 2	98.3
	Cluster 2	99.0
	Cluster 3	98.9

Figure 48: Normalized melting curves give different G151R cluster with a percentage of confidence of 99%

One of these experiments was performed using 53°C as annealing temperature to evaluate the reproducibility of the experiments with a different temperature. Figure 49 shows that the result obtained with 53°C was similar to that obtained with 55°C, as reported in Figure 47. HRM analysis clearly showed the presence of L168R mutation in cf-DNA isolated from left adrenal vein and, therefore, from the APA side. The fact that cf-DNA isolated from left side clusters with the left adrenal tissue strongly supports the working hypothesis of this study that KCNJ5 mutations can be detected not only in APA, but also in circulating blood.

Figure 49: Normalized melting curves give different L168R cluster



Content	Sample	Cluster	Percent Confidence
Unkn		Cluster 1	99.3
Unkn		Cluster 1	98.3
Unkn		Cluster 1	99.3
Unkn		Cluster 1	83.4
Unkn		Cluster 2	94.5
Unkn		Cluster 2	96.0
Unkn		Cluster 3	99.2

Discussion

We developed in our laboratory a novel method based on Taq-man probes to detect somatic KCNJ5 mutations in the APA tissue. This novel method can be proposed as an alternative to Sanger sequencing, which is time consuming and expensive technique. When compared the results obtained from the Taq-man probes-based technique to those obtained from the gold standard Sanger technique, we did not find any misclassification of mutated and wild-type APAs, thereby providing evidence of diagnostic accuracy of the new method.

The growing interest for the early diagnosis of mutated tumours, and the continuous research of a predictive method that supports AVS to subtype the two main forms of PA, prompted us to isolate cf-DNA from blood of the adrenal veins and detect KCNJ5 mutations in cf-DNA. By applying Taq-man probes-based technique and HRM analysis we were able to detect KCNJ5 mutation in cf-DNA isolated from the adrenal vein that drained blood from a mutated APA. In fact, HRM analysis clearly showed the presence of L168R mutation in cf-DNA isolated from left adrenal vein of one patient with an APA harboring L168R mutation in the left adrenal gland. The fact that cf-DNA isolated from left side clusters with the left adrenal tissue strongly supports the working hypothesis of this study that KCNJ5 mutations can be detected not only in APA, but also in circulating blood. Some methodologic aspects deserve interest because they were crucial for cf-DNA detection in plasma. For example, since cf-DNA levels are very low in blood under physiologic conditions or conditions associated with benign tumors, we modified our Taq-man protocol until reaching the best operative conditions that allowed us to analyze very tiny amounts of cf-DNA.

This study also suggests that the major mechanism by which cells release cf-DNA into the bloodstream is apoptosis. Cf-DNA isolated from plasma of adrenal veins and inferior vena cava was significantly lower than that found in peripheral blood of patients with stomach cancer. Progression of tumour and occurrence of metastases are factors usually associated with long circulating DNA fragments, which presumably derive from necrotic debris. In contrast, the release of fragments with minor length from apoptotic cells of wild type tissue and mutated APA could be related to the physiologic or pathophysiologic cellular turnover, respectively, not to necrotic death. Cf-DNA fragments are usually generated at the end of apoptosis process in the cells, when the proteases and nuclear endonucleases act on chromatin generating fragments of about 200 bp. Apoptosis involves all tissues, even though to different extent, and therefore it is reasonable to contend occurrence of apoptosis also in the adrenal tissue.

Hence, the new strategy based on Taq-man probes and HRM analysis could be useful not only for detecting gene mutations, but also to gain a deep insight into pathophysiologic mechanisms underlying the development of APA.

Conclusions and perspectives

The results of this study showed that somatic mutations in KCNJ5 gene could be detected in the APA tissue using highly specific TAQ-MAN probes. This approach developed in our laboratory avoids use of the time-consuming Sanger sequencing, and also allows detection of G151R and L168 mutations at the same time and in the same PCR sample. TAQ-MAN probes-based technique associated with HRM analyses seems a promising approach even for the detection of KCNJ5 mutations in cf-DNA isolated from the adrenal vein that drains blood from the mutated APA, suggesting that KCNJ5 mutations may be revealed before adrenalectomy. Since APAs harboring KCNJ5 mutation were found to be associated with higher aldosterone levels than wild-type APAs, an early detection of the mutation could be useful to select patients to address to AVS.

The relatively low integrity index of cf-DNA suggests that DNA is released from the APA cells that undergo apoptosis and, therefore, provides novel information on pathophysiology of the APA.

Hence, these findings collectively would lay the foundations for the development of a strategy to pinpoint the mutations in KNJ5 gene. Furthermore, this strategy could be applied to detect KCNJ5 mutations involved in germline heterozygous mutations responsible for hereditary form of hyperaldosteronism (FH-3).

Bibliography

Funder, J. W. *et al.* Case detection, diagnosis, and treatment of patients with primary aldosteronism: an endocrine society clinical practice guideline. *J. Clin. Endocrinol. Metab.* **93**, 3266–3281 (2008).

Rosenquist, K. J. & Dluhy, R. G. Adrenal gland: Uncertainty in the selective use of adrenal vein sampling. *Nat. Rev. Endocrinol.* **7**, 442–443 (2011).

Boukroun, S. *et al.* KCNJ5 mutations in aldosterone producing adenoma and relationship with adrenal cortex remodeling. *Mol. Cell. Endocrinol.* **371**, 221–227 (2013).

Seccia, T. M. *et al.* Adrenocorticotrophic hormone stimulation during adrenal vein sampling for identifying surgically curable subtypes of primary aldosteronism comparison of 3 different protocols. *Hypertension* **53**, 761–766 (2009).

Stewart, P. M. & Allolio, B. Adrenal vein sampling for Primary Aldosteronism: time for a reality check. *Clin. Endocrinol. (Oxf)*. **72**, 146–148 (2010).

Calhoun, D. a., Nishizaka, M. K., Zaman, M. a., Thakkar, R. B. & Weissmann, P. Hyperaldosteronism among black and white subjects with resistant hypertension. *Hypertension* **40**, 892–896 (2002).

Jahr, S. *et al.* DNA Fragments in the Blood Plasma of Cancer Patients : Quantitations and Evidence for Their Origin from Apoptotic and Necrotic Cells DNA Fragments in the Blood Plasma of Cancer Patients : Quantitations and Evidence for Their Origin from Apoptotic and Necr. *Cancer Res.* **61**, 1659–1665 (2001).

Umetani, N. *et al.* Prediction of breast tumor progression by integrity of free circulating DNA in serum. *J. Clin. Oncol.* **24**, 4270–4276 (2006).

Rossi, G. P. D. Diagnosis and treatment of primary aldosteronism. *Rev. Endocr. Metab. Disord.* **12**, 27–36 (2011).

Azizan, E. a B. *et al.* Microarray, qPCR, and KCNJ5 sequencing of aldosterone-producing adenomas reveal differences in genotype and phenotype between zona glomerulosa- and zona fasciculata-like tumors. *J. Clin. Endocrinol. Metab.* **97**, 819–829 (2012).

Azizan, E. a B. *et al.* Somatic mutations in ATP1A1 and CACNA1D underlie a common subtype of adrenal hypertension. *Nat. Genet.* **45**, 1055–60 (2013).

Monticone, S. *et al.* A novel Y152C KCNJ5 mutation responsible for familial hyperaldosteronism type III. *J. Clin. Endocrinol. Metab.* **98**, 1861–1865 (2013).

Rossi, G. P. *et al.* A Prospective Study of the Prevalence of Primary Aldosteronism in 1,125 Hypertensive Patients. *J. Am. Coll. Cardiol.* **48**, 2293–2300 (2006).

Young, W. F. *et al.* Role for adrenal venous sampling in primary aldosteronism. *Surgery* **136**, 1227–1235 (2004).

Azizan, E. a B. *et al.* Somatic mutations affecting the selectivity filter of KCNJ5 are frequent in 2 large unselected collections of adrenal aldosteronomas. *Hypertension* **59**, 587–591 (2012).

Rossi, G. P. *et al.* Identification of the etiology of primary aldosteronism with adrenal vein sampling in patients with equivocal computed tomography and magnetic resonance findings: Results in 104 consecutive cases. *J. Clin. Endocrinol. Metab.* **86**, 1083–1090 (2001).

Bassett, M. H., Suzuki, T., Sasano, H., White, P. C. & Rainey, W. E. The orphan nuclear receptors NURR1 and NGFIB regulate adrenal aldosterone production. *Mol. Endocrinol.* **18**, 279–290 (2004).

Charmandari, E. *et al.* A novel point mutation in the KCNJ5 gene causing primary hyperaldosteronism and early-onset autosomal dominant hypertension. *J. Clin. Endocrinol. Metab.* **97**, 1532–1539 (2012).

Rossi, G. P. *et al.* An expert consensus statement on use of adrenal vein sampling for the subtyping of primary aldosteronism. *Hypertension* **63**, 151–160 (2014).

Mcmahon, G. T., Dluhy, R. G. & Aldosteronism, G. Glucocorticoid-Remediable Aldosteronism. **48**, (2004).

Chen, Z., Fadiel, a., Naftolin, F., Eichenbaum, K. D. & Xia, Y. Circulation DNA: Biological implications for cancer metastasis and immunology. *Med. Hypotheses* **65**, 956–961 (2005).

Wang, B. G. *et al.* Increased plasma DNA integrity in cancer patients. *Cancer Res.* **63**, 3966–3968 (2003).

Mulatero, P. *et al.* Long-term cardio- and cerebrovascular events in patients with primary aldosteronism. *J. Clin. Endocrinol. Metab.* **98**, 4826–33 (2013).

Kempers, M. J. E. *et al.* Systematic review: diagnostic procedures to differentiate unilateral from bilateral adrenal abnormality in primary aldosteronism. *Ann. Intern. Med.* **151**, 329–337 (2009).

Xekouki, P. *et al.* KCNJ5 mutations in the National Institutes of Health cohort of patients with primary hyperaldosteronism: An infrequent genetic cause of Conn's syndrome. *Endocr. Relat. Cancer* **19**, 255–260 (2012).

Zennaro, M. C., Jeunemaitre, X. & Boulkroun, S. Integrating genetics and genomics in primary aldosteronism. *Hypertension* **60**, 580–588 (2012).

Kuppusamy, M. *et al.* A Novel KCNJ5-insT149 Somatic Mutation Close to, but Outside, the Selectivity Filter Causes Resistant Hypertension by Loss of Selectivity for Potassium. *J. Clin. Endocrinol. Metab.* **99**, jc20141927 (2014).

Lenzini, L. & Rossi, G. P. ScienceDirect The molecular basis of primary aldosteronism : from chimeric gene to channelopathy. (2014).

Sánchez-Céspedes, M. *et al.* Detection of chromosome 3p alterations in serum DNA of non-small-cell lung cancer patients. *Ann. Oncol.* **9**, 113–116 (1998).

Beuschlein, F. Regulation of aldosterone secretion: From physiology to disease. *Eur. J. Endocrinol.* **168**, 85–93 (2013).

Boukroun, S. *et al.* Prevalence, clinical, and molecular correlates of KCNJ5 mutations in primary aldosteronism. *Hypertension* **59**, 592–598 (2012).

Van Der Vaart, M. & Pretorius, P. J. Circulating DNA: Its origin and fluctuation. *Ann. N. Y. Acad. Sci.* **1137**, 18–26 (2008).

Monticone, S. *et al.* Effect of KCNJ5 mutations on gene expression in aldosterone-producing adenomas and adrenocortical cells. *J. Clin. Endocrinol. Metab.* **97**, 1567–1572 (2012).

Hannemann, a. *et al.* Screening for primary aldosteronism in hypertensive subjects: Results from two German epidemiological studies. *Eur. J. Endocrinol.* **167**, 7–15 (2012).

Beuschlein, F. *et al.* Somatic mutations in ATP1A1 and ATP2B3 lead to aldosterone-producing adenomas and secondary hypertension. *Nat. Genet.* **45**, 440–4, 444e1–2 (2013).

Rossi, G. P. *et al.* The adrenal vein sampling International study (avis) for identifying the major subtypes of primary aldosteronism. *J. Clin. Endocrinol. Metab.* **97**, 1606–1614 (2012).

Taguchi, R. *et al.* Expression and mutations of KCNJ5 mRNA in Japanese patients with aldosterone-producing adenomas. *J. Clin. Endocrinol. Metab.* **97**, 1311–1319 (2012).

Guagliardo, N. a., Yao, J., Hu, C. & Barrett, P. Q. Minireview: Aldosterone biosynthesis: Electrically gated for our protection. *Endocrinology* **153**, 3579–3586 (2012).

Scholl, U. I. *et al.* Hypertension with or without adrenal hyperplasia due to different inherited mutations in the potassium channel KCNJ5. *Proc. Natl. Acad. Sci.* **109**, 2533–2538 (2012).

Williams, T. A. *et al.* Somatic ATP1A1, ATP2B3, and KCNJ5 mutations in aldosterone-producing adenomas. *Hypertension* **63**, 188–195 (2014).

Pinzani, P. *et al.* Circulating cell-free DNA in plasma of melanoma patients: Qualitative and quantitative considerations. *Clin. Chim. Acta* **412**, 2141–2145 (2011).

Benesova, L. *et al.* Mutation-based detection and monitoring of cell-free tumor DNA in peripheral blood of cancer patients. *Anal. Biochem.* **433**, 227–234 (2013).

Kirsch, C., Weickmann, S., Schmidt, B. & Fleischhacker, M. An improved method for the isolation of free-circulating plasma DNA and cell-free DNA from other body fluids. *Ann. N. Y. Acad. Sci.* **1137**, 135–139 (2008).

Thierry, A. R. *et al.* Origin and quantification of circulating DNA in mice with human colorectal cancer xenografts. *Nucleic Acids Res.* **38**, 6159–6175 (2010).

Mouliere, F. *et al.* High fragmentation characterizes tumour-derived circulating DNA. *PLoS One* **6**, (2011).

Bettegowda, C. & Sausen, M. Detection of Circulating Tumor DNA in Early- and Late-Stage Human Malignancies. *Sci. Transl. ...* **6**, (2014).

Hao, T. B. *et al.* Circulating cell-free DNA in serum as a biomarker for diagnosis and prognostic prediction of colorectal cancer. *Br. J. Cancer* 1482–1489 (2014). doi:10.1038/bjc.2014.470

Sutherland, D. J., Ruse, J. L. & Laidlaw, J. C. Hypertension, increased aldosterone secretion and low plasma renin activity relieved by dexamethasone. *Can. Med. Assoc. J.* **95**, 1109–1119 (1966).

Al-Salameh, A., Cohen, R. & Desailoud, R. Overview of the genetic determinants of primary aldosteronism. *Appl. Clin. Genet.* **7**, 67–79 (2014).

Amar, L., Lorthioir, a., Azizi, M. & Plouin, P.-F. PROGRESS IN PRIMARY ALDOSTERONISM: Mineralocorticoid antagonist treatment for aldosterone-producing adenoma. *Eur. J. Endocrinol.* **172**, R125–R129 (2014).

McMahon GT, Dluhy RG. Glucocorticoid-remediable aldosteronism. *Cardiol Rev.* 2004;12(1):44–48.

Lifton RP, Dluhy RG, Powers M, et al. A chimaeric 11 beta-hydroxylase/aldosterone synthase gene causes glucocorticoid-remediable aldosteronism and human hypertension. *Nature.* 1992;355(6357):262–265.